2013-12-12

Identification of the Binding Partners for HspB2 and CryAB Reveals Myofibril and Mitochondrial Protein Interactions and Non-Redundant Roles for Small Heat Shock Proteins

Kelsey Murphey Langston
Brigham Young University - Provo

Identification of the Binding Partners for HspB2 and CryAB Reveals Myofibril and Mitochondrial Protein Interactions and Non-Redundant Roles for Small Heat Shock Proteins

Kelsey Langston

A thesis submitted to the faculty of
Brigham Young University
in partial fulfillment of the requirements for the degree of

Master of Science

Julianne H. Grose, Chair
William R. McCleary
Brian Poole

Department of Microbiology and Molecular Biology

Brigham Young University

December 2013

ABSTRACT

Identification of the Binding Partners for HspB2 and CryAB Reveals Myofibril and Mitochondrial Protein Interactors and Non-Redundant Roles for Small Heat Shock Proteins

Kelsey Langston

Department of Microbiology and Molecular Biology, BYU

Master of Science

Small Heat Shock Proteins (sHSP) are molecular chaperones that play protective roles in cell survival and have been shown to possess chaperone activity. As such, mutations in this family of proteins result in a wide variety of diseases from cancers to cardiomyopathies. The sHSPs Beta-2 (HspB2) and alpha-beta crystalline (CryAB) are two of the ten human sHSPs and are both expressed in cardiac and skeletal muscle cells. A heart that cannot properly recover or defend against stressors such as extreme heat or cold, oxidative/reductive stress, and heavy metal-induced stress will constantly struggle to maintain efficient function. Accordingly, CryAB is required for myofibril recovery from ischemia/reperfusion (I/R) and HspB2 is required I/R recovery as well as efficient cardiac ATP production. Despite these critical roles, little is known about the molecular function of these chaperones. We have identified over two hundred HspB2-binding partners through both yeast two-hybrid and copurification approaches, including interactions with myofibril and mitochondrial proteins. There is remarkable overlap between the two approaches (80%) suggesting a high confidence level in our findings. The sHSP, CryAB, only binds a subset of the HspB2 interactome, showing that the HspB2 interactome is specific to HspB2 and supporting non-redundant roles for sHSPs. We have confirmed a subset of these binding partners as HspB2 clients via in vitro chaperone activity assays. In addition, comparing the binding patterns and activity of sHSP variants in comparison to wild type can help to elucidate how variants participate in causing disease. Accordingly, we have used Y2H and in vitro chaperone activity assays to compare the disease-associated human variants R120GCryAB and A177PHspB2 to wild type and have identified differences in binding and chaperone function. These results not only provide the first molecular evidence for non-redundancy of the sHSPs, but provides a useful resource for the study of sHSPs in mitochondrial and myofibril function.

Keywords: small heat shock proteins (sHSP), HspB2 (MKBP), HspB5 (CryAB), R120G, A177P, molecular chaperones, myocardial maintenance strategies, mitochondria, proteostasis

TABLE OF CONTENTS

LIST OF TABLES

LIST OF FIGURES

SPECIFIC AIMS

HspB2 and CryAB (HspB5) are small Heat Shock Proteins (sHSPs) that are highly expressed in cardiac muscle and appear to maintain mitochondrial function and play protective roles during cardiac stress. Both HspB2 and CryAB function as protein chaperones to help maintain protein fold or refold proteins during stress. Alterations in sHSP function have been shown to lead to a wide variety of diseases with a mutation in the CryAB gene (denoted R120GCryAB) causing cardiomyopathy in both humans as well as mice. The molecular mechanisms by which HspB2 and CryAB maintain and protect the heart are currently unknown, including involved pathways and substrates. Identifying and further characterizing the protein binding partners for these sHSPs will help elucidate their molecular role and may explain how the R120G mutant causes disease.

Our first hypothesis is that HspB2 will interact with a number of human cardiac proteins, including proteins associated with the actin cytoskeleton and the mitochondrion. HspB2 has been shown to localize to the neuromuscular junction and to the cross sections of individual myofibrils at the Z-membrane. Furthermore, HspB2 deficiency in mouse hearts leads to a reduction of mitochondrial fatty acid beta-oxidation, ATP production, and alterations in the transcript levels of several metabolic and mitochondrial regulator genes. HspB2 has been found to interact with DMPK, a protein kinase necessary for the maintenance of skeletal muscle structure and function, but has not previously been shown to interact with any mitochondrial substrates, metabolic regulators, or myofibril proteins. Our first Aim was to identify human myocardial proteins that interact with HspB2 and delineate protein-interaction networks with which HspB2 may be involved in order to help elucidate specific molecular functions for this sHSP within the human heart.

Our second hypothesis is that HspB2 displays chaperone activity by preventing the erroneous aggregation of specific unfolding proteins during conditions of stress. Consistent with our hypothesis for specificity, HspB2 has been shown to prevent the DTT-induced protein aggregation of insulin and the heat-induced aggregation of yeast alcohol dehydrogenase, but only partially prevents the heat-induced aggregation of citrate synthase. Our second aim was to verify a subset of the HspB2-cardiac binding partners as clientele through in vitro chaperone activity assays. Due to our particular interest in HspB2's mitochondrial role, we focused our assays on a subset of mitochondrial proteins expressed in the myocardium. Our goal was to ascertain whether HspB2 acts to prevent aggregation and maintain protein function under conditions of stress.

Our third hypothesis is that WTCryAB and the mutated R120GCryAB proteins associate with interacting-proteins differently, leading to the ineffectual building and maintenance of cardiac muscle structure when the mutated CryAB form is present. A mutation in the CryAB gene denoted R120GCryAB results in increased expression of glucose-6-phosphate (G6PDH), consequentially increased cellular levels of NADPH, and ultimately the NADPH-dependent inducement of cardiomyopathy in mice. Our third aim was to determine if CryAB and R120GCryAB displayed differential chaperone activity. The results will help to elucidate the molecular mechanisms by which CryAB maintains function and by which R120GCryAB causes disease.

Specific Aim I: Complete the identification of novel binding partners for HspB2 by utilizing the yeast two-hybrid assay and delineate protein-interaction networks with which HspB2 may be involved by performing bioinformatic analyses.

Specific Aim II: Verify the role of HspB2 as a chaperone and its ability to maintain protein function through the use of in vitro chaperone and enzyme activity assays.

Specific Aim III: Compare the nature of human cardiac protein interactions with WTCryAB and R120GCryAB sHSPs through the use of in vitro chaperone activity assays.

CHAPTER ONE: HspB2 Responds to Cardiac Stress

INTRODUCTION

Only about half of all cardiomyocytes are replaced in a human lifespan, making cardiac maintenance strategies imperative to human health. The continuous beating of cardiac cells necessitates a large mitochondrial residence. In fact, mitochondria contribute to 35-40% of the cardiac volume as opposed to 2% of skeletal muscle volume [1, 2]. Increased heart rate, which occurs during exercise or other strenuous activities, increases the metabolic demand of cardiac cells. During times of increased metabolic demand , cardiomyocytes will shift from non-carbohydrate (fatty acid) to carbohydrate (glucose) metabolism [3]. Mitochondria are the largest cellular contributors to reactive oxygen species (ROS) and reactive nitrogen species (RNS) production, developed particularly from electrons that escape the electron transport chain and associate directly with oxygen, water, or other molecules. Hence, the elevated need for metabolic activity due to constant beating and during times of increased strenuous activity results in a heightened production of ROS/RNS and a struggle to maintain REDOX balance as oxidative and reductive damage ensues. Cardiomyocytes need to be able to protect themselves from the repercussions of an increased energetic demand.

Maintaining protein homeostasis, also termed "proteostasis," is a key goal of cardiac maintenance strategies. In proteostasis, protein synthesis, organization, folding and degradation are being continuously coordinated to allow for a healthy cellular environment [4]. When cardiac cells are subjected to deleterious conditions and events of stress, maintaining proteostasis becomes particularly difficult. Heart attack, stroke, and plaque blockages can lead to both ischemia/reperfusion injuries of myocardial cells as well as mechanical pressure-overload stress.

Such deleterious events can lead to an explosion of ROS/RNS production, mitochondrial deterioration, cytoskeletal disruption, membrane lipid peroxidation, and events of apoptosis and necrosis. Temperature extremes such as increased heat can cause proteins and enzymes to denature and aggregate, thereby constraining normal cellular function and resulting in cellular damage. Molecular chaperones, including small Heat Shock Proteins (sHSPs) such as HspB2, play considerable roles in maintaining proteostasis and conferring stress resistance. This review will explore what is currently known about the small heat shock protein HspB2, including its role in cardiac maintenance.

SMALL HEAT SHOCK PROTEINS PLAY CONSERVATIONAL ROLES IN CELL SURVIVAL

There are ten known human sHSPs that range in size from 12-43 kDa and contain a conserved α-crystallin domain near the C-terminus as well as a more variable N-terminal region [5]. While some sHSPs are constitutively expressed, stressors including heat extremes, oxidative stress, and the presence of misfolded proteins or polypeptide aggregation have been shown to induce expression of some sHSPs. Conserved from yeast to man, these proteins have been implicated in a variety of processes including cytoskeletal assembly, remodeling and stabilization, actin and intermediate filament dynamics, apoptosis inhibition, cellular redox state maintenance, modulation of membrane fluidity and vasorelaxation. In addition, sHSPs serve as structural proteins in eye lens and sperm tail [6-17]. Most sHSPs possess chaperone activity and bind to misfolded or denatured proteins in an ATP-independent manner to prevent protein aggregation. They can also transfer proteins to larger ATP-dependent heat shock proteins for refolding or subsequent degradation (for recent reviews see [16, 18]).

In order to prevent protein aggregation of denaturing or misfolded proteins, sHSPs oligomerize into homo- or heteromeric complexes through ionic and hydrophobic interactions between sHSP monomers. These sHSPs may form either hollow spheres around misfolding proteins or disc-like structures capable of dimer dissociation and subsequent substrate binding [5, 19, 20]. These monomers will first dimerize, tetramerize, and then undergo further oligomerization. The α-crystallin domain is located near the C-terminus, is folded into a β-sandwich conformation comprised of two β-sheets, and is essential for dimerization. Different dimer interfaces have been reported. The β-6 strand of both monomers can be incorporated into a β-sheet of the opposing monomer. Another dimer interface includes the elongated β-7 strands of the monomers being incorporated into the opposing monomer's β-sheet in such a way as to create a single, continuous β-sheet between the two monomers [19, 21, 22]. Oligomers can be formed through the association of a somewhat flexible C-terminal extension with the α-crystallin domain of other sHSP monomers. The more variable N-terminus of sHSPs consists of a flexible arm that may contain α-helices involved in pairwise interactions separate from the dimers formed through the α-crystallin domain [20]. Oligomerization of sHSPs can be regulated by several processes. Phosphorylation events have been shown to alter the oligomeric states of some sHSPs [23, 24]. Furthermore, as proteins denature, hydrophobic residues are exposed that may associate with the hydrophobic regions of sHSPs. In addition to being regulated through oligomerization, sHSPs must recognize their substrates in order to elicit protective effects. Although oligomerization sites have been identified for sHSPs, there is no single substrate-binding site that has been identified. Rather, there are likely to be several substrate-interacting sites per substrate that may be substrate-dependent (for a recent review see [18]).

THE SMALL HEAT SHOCK PROTEIN HSPB2

Genetic Features and Expression Patterns

The gene encoding HspB2 was discovered during an attempt to identify regulatory elements of HspB5 (CryAB) and then rediscovered a year later as a protein that binds to and activates Myotonic Dystrophy Protein Kinase (DMPK) [25, 26]. As a result, alternative names for HspB2 have been coined including Myotonic Dystrophy Protein Kinase Binding Protein (MKBP). The gene encoding HspB2 can be found in all vertebrates for which there is sequence data, with the exception of birds and reptiles. Located on human chromosome 11, the HspB2 gene is situated 958 base pairs upstream of HspB5 and is oriented in a head-to-head fashion with HspB5. The head-to-head orientation of these small heat shock proteins may be the results of either an inverted duplication or translocation event [27], after which the two proteins diverged further. They currently share 41% amino acid identity and 56% similarity, suggesting functional differences. The mRNA transcript of the HspB2 gene is at least 844 base pairs in length excluding the polyA tail, is composed of two exons and one intron, and encodes a highly conserved α-crystallin domain that is shared by all members of the sHSP family [5, 25]. While comparing the rat homologue of HspB2 to human, Iwaki et al. observed that the intron region of rat HspB2 is 94 base pairs shorter, but that the coding region possesses 92% identity to the human homologue of HspB2. Furthermore, the amino acid sequence of the rat and human HspB2 homologues share 97% identity, advocating HspB2 as a highly conserved protein [25] and providing further evolutionary support for functional differences between HspB2 and HspB5.

Differential expression of HspB2 and HspB5 provides further support for differential function. While HspB2 and HspB5 may share some promoter elements, they have two different transcriptional start sites. It seems unlikely that they share the two heat shock elements (HSEs)

located upstream of HspB5 that allow increased transcription as a result of heat shock and very likely that they share the E-boxes which are responsible for protein expression in muscle tissue [25]. Heat stress results in increased expression of HspB5, however, expression of HspB2 in not induced by heat shock [25, 26, 28]. While HspB2 is not induced by heat shock, other stressors and factors have been shown to result in increased HspB2 expression. Methamphetamine preconditioning may provide neuroprotection in rodents by up-regulating HspB2 transcription [29]. Reduced DMPK levels also result in increased HspB2 expression [28]. Furthermore, stretch stimulation in neonatal mouse cardiomyocytes causes increased HspB2 protein levels, but not HspB5 levels, indicating a possible HspB2-specific response to mechanical stress [26]. HspB2 protein levels in the infant rat myocardium rapidly increase after birth, rising to a 3-fold increase at 1 wk in comparison to fetus levels, and rapidly decreasing at 13 wk. Human neonatal myocardium shows similar age-dependency, being high in the neonatal heart and sharply decreasing after 2-11 mo, remaining low between 11 and 69 y of age [30]. The myogenic factor MyoD has been shown to induce HspB2 expression during muscle differentiation [28]. There are two conserved E-boxes located roughly 140 and 166 bps upstream of the HspB2 transcription start site that serve as binding sites for a family of muscle-specific transcription factors called the MyoD family.

Northern blot analysis reveals that HspB2 is expressed primarily in skeletal muscle and heart tissue, but to a lesser extent than HspB5 [25]. There are two DNase I hypersensitive regions located upstream of HspB5, which are general indications that the DNA at this location is nucleosome-free, suggesting a greater likelihood of expression [25]. HspB2 has also been detected at low levels in prostate, ovary, intestine, and colon tissue [28]. Expression of HspB2 is higher in cardiac and soleus muscle, which are slow-twitch muscles and have a higher

mitochondrial content, in comparison to femoral and gastrocnemius muscle, which are fast-twitch muscle and have a lower mitochondrial content. This finding suggests a potential relationship between HspB2 and the mitochondria [31].

Cellular Localization

HspB2 may associate loosely with the mitochondrial outer membrane under normal conditions and relocalizes to the mitochondrial membrane and nucleus upon heat shock. After fractionating differentiated mouse myoblast cells, Nakagawa et al. discovered HspB2 mainly in the post mitochondrial supernatant and not in the mitochondrial fraction. They then examined the subcellular localization of HspB2 in different cell types via immunofluorescence and report HspB2 in cytosolic granules and at the outer membrane of the mitochondria in a cell line derived from a human malignant glioma [31]. In addition, mild heat treatment increases the amount of HspB2 that colocalizes with the mitochondria in differentiated mouse myoblast cells, as determined through fractionating heat-treated cells and detecting increased levels of HspB2 in the mitochondrial fraction. This mitochondrial association is consistent with recent phenotypic evidence linking HspB2 to ATP production [32]. Increased levels of HspB2 were also found to localize with the nucleus of heat-treated differentiated mouse myoblast cells in comparison to cells kept at 37°C [31]. However, Ishiwata et al. were not able to detect HspB2 in the mitochondrial fraction derived from murine cardiac cells under normal or heat shock conditions [32]. HspB2 may loosely associate with the mitochondrial outer membrane during normal physiological and heat stress conditions, but not in high enough concentrations to be detected in the murine myocardium.

In addition to mitochondrial and nuclear relocation, heat stress, ischemia and possibly oxidative stress, but not pressure overload stress, results in the relocalization of HspB2 from the cytosol to the cytoskeleton. Under normal physiological conditions, 50% of HspB2 is found in the soluble fraction of rat skeletal muscle and relocates to the insoluble fraction upon heat stress [26]. Subcellular immunolocalization assays of HspB2 in human skeletal muscle show HspB2 localization at the neuromuscular junction, the junction between a nerve fiber and the muscle it supplies, and to the cross sections of individual myofibrils at the Z-membrane where the HspB2-binding protein DMPK resides [26]. An immunofluorescence analysis performed on the rat neonatal myocardium reveals a similar pattern with HspB2 protein localization at the Z lines and intercalated discs, suggesting a possible role of HspB2 in protecting the actin cytoskeleton of the neonatal heart against oxidative stress [30]. In addition, ischemic stress in rat heart causes HspB2 to translocate from the cytosol to the myofibril fraction [33, 34]. The myofibril relocalization of HspB2 is stress-specific since Ishiwata et al. did not observe Z-band localization in response to pressure overload stress in mice [32].HspB2 does not, however, exhibit "a myotube-specific association with actin bundles," as seen with HspB5 or HspB1, in mouse myoblast cell cultures [28]. In contrast to the data from human and rat tissue, HspB2 does not appear to colocalize with actin filaments, intermediate filaments, or microtubules in a cell line derived from a human malignant glioma [31]. This difference in localization may be attributed to the use of cancer cell lines instead of type tissues.

The mechanism by which HspB2 relocates during periods of cellular stress is currently unknown. Cellular stressors such as ischemia and reperfusion can result in the activation of several protein kinases including p38 MAP kinase and protein kinase C [35-37]. These kinases can then phosphorylate and activate sHSPs. The delta form of protein kinase C phosphorylates

HspB1 [38], as does the protein kinase p38 MAPK when activated by oxidative stress in vascular endothelial cells, resulting in microfilament reorganization [39]. The sHSP HspB5 is also phosphorylated by p38 MAPK upon cytoskeletal disorganization and causes HspB5 to relocate to cytoskeletal components [40]. However, neither protein kinase C nor p38 MAPK affects the ability of HspB2 to translocate under ischemic conditions. In fact, no change in the phosphorylation state of HspB2 is detected during ischemic conditions [34]. Hence, translocation of HspB2 during ischemia does not ensue as a result of HspB2-phosphorylation by either of these two proteins and appears to be triggered by a mechanism other than phosphorylation [34].

Molecular Properties of HspB2

The HspB2 protein is 182 amino acids in length with an estimated molecular mass of 20,233-20,295 Da and is the most divergent protein among the small heat shock proteins, sharing only 30% sequence identity to the other human sHSPs. The region of greatest sequence similarity occurs in the α-crystallin domain located near the C-terminus, where at least 42% sequence identity is shared [26]. No additional similarity is observed between the C-terminus of HspB2 and the other human sHSPs. Prabhu et al. studied the secondary structure of HspB2 by far-UV circular dichroism spectroscopy, analyzing the spectrum using the CDNN program, and report that HspB2 contains 3.4% helix, 50.5% β-sheet, and 53.9% random coil [41]. The tertiary structure of HspB2 has been suggested to be highly compact with a tryptophan residue at the 130th amino acid position being solvent-exposed and highly accessible [41]. HspB2 undergoes temperature-induced conformational changes at temperatures ranging from 25 to 60°C, but does not begin to denature until after 55°C leading to a complete loss of secondary structure at 60°C

[41, 42]. Hence, HspB2 may begin to relinquish tertiary structure, but will maintain secondary structure even at high physiological temperature extremes.

HspB2 displays alternate oligomeric organization under different conditions including hetero-oligomers involving other sHSPs. HspB2 oligomers exhibit subunit exchange and can possess a broad range of multimeric species that are HspB2-concentration-dependent [41]. In addition, the HspB2 oligomeric complex compositions may be slightly different between the complexes found in skeletal muscle and cardiomyocytes because the molecular masses are different in these tissue types [26].

HspB2 has been shown to form hetero-oligomers with HspB3, HspB5 (CryAB), HspB6 (p20), or HspB8 [28, 42, 43][44]. HspB8 is also known to associate with HspB1, HspB6, HspB7 and itself, while HspB3 is only known to associate with HspB2. The hetero-oligomers formed by HspB2 and HspB3 maintain a strict 3:1 HspB2/B3 subunit ratio. The size of the resulting hetero-oligomer complex increases proportionally to the concentration and availability of HspB2 and HspB3 and can remain stable up to 40°C. As a consequence, the hetero-oligomers may consist of 4, 8, 12, 16, 20, or 24 subunits, with the tetramer being the most abundant oligomeric species formed [42]. The HspB2/B3 complexes cannot interact with complexes formed from HspB1, HspB5, and HspB6 while HspB2 homo-oligomers can [42]. HspB2 has been suggested to mostly associate with HspB3, leaving little HspB2 remaining to associate with HspB6 in muscle tissue [42]. Suzuki et al. failed to detect an interaction between HspB2 and HspB5 or HspB1 in mouse cardiomyocytes through gel filtration and immunoblotting analysis [26]. Despite the clear evidence for hetero-oligomers, the role they play in regulating HspB2 function, including chaperone activity and clientele is largely unknown.

Chaperone Activity and Other Protein Interactions of HspB2

HspB2 may associate with denaturing protein in part through hydrophobic interactions. Hydrophobic interactions are believed to be important for molecular chaperone-like activity and while HspB2 has accessible hydrophobic surfaces, HspB5 has significantly more [41]. The inference is that HspB5 has better chaperone-like activity than HspB2, at least under normal physiological conditions. Increasing temperatures that cause HspB2 to begin to unfold may increase HspB2 chaperone capabilities by exposing greater hydrophobicity. In support of this hypothesis, as temperatures elevate to heat shock conditions, HspB2 becomes more active in performing chaperone function [41]. In addition to activation by temperature, the chaperone activity of HspB2 exhibits protein-specificity as well. While HspB2 prevents the DTT-induced protein aggregation of insulin and the heat-induced aggregation of yeast alcohol dehydrogenase (48°C), HspB2 only partially prevents the heat-induced aggregation of citrate synthase (43°C) [41]. HspB2 is also able to prevent the amyloid fibril formation of α-synuclein, a formation involved in some neurodegenerative diseases [41]. In contrast, the HspB2/B3 complex is relatively non-hydrophobic and does not help to prevent the aggregation of DTT-denatured insulin or heat-induced aggregation of citrate synthase while HspB5 is able to do so [42]. In addition, while HspB5 is able to aid in growth recovery of heat-shocked E. coli cells, the HspB2/B3 complex is unable to do so [42]. Hence, HspB3 may negatively regulate HspB2 chaperone activity.

HspB2 is the only sHSP known to bind and activate myotonic dystrophy protein kinase (DMPK), a serine/theonine protein kinase involved in muscle structure maintenance and function [28, 41]. DMPK binds to the α-crystallin domain of HspB2 and HspB2 binds to the kinase domain of DMPK, thereby activating the kinase activity of DMPK and conferring

thermoresistance. HspB2 may also assist DMPK in autophosphorylating itself, causing kinase activation. By suppressing the heat-induced inactivation of DMPK, HspB2 is able to help maintain muscle structure and function [26]. In addition to HspB2's role in myofibril maintenance, recent functional evidence suggests a role for HspB2 in mitochondrial function.

PHENOTYPES ASSOCIATED WITH HSPB2

The sHSP family is difficult to study in part due to overlapping function of the ten mammalian sHSPs. However, phenotypic evidence from single sHSP knockout mice has begun to uncover their individual roles. For HspB2, initial studies were performed in mice lacking both HspB2 and HspB5 because the targeting strategy employed to create a global HspB5 specific knockout mouse line disrupted the promoter region required for HspB2 expression [45]. A study performed by Pinz et al. over-expressed HspB2 in the Double Knock-Out (DKO) mouse line in order to determine the effects of HspB2-specific deficiency [33]. A specific HspB2 knockout mouse line was created only recently in order to observe the effects of myocardial HspB2 deficiency in an otherwise wild type background [32]. A summary of the effects of HspB5/HspB2 DKO and HspB2 deficiency in mouse hearts can be found in Table 1.1.

Knockout Effects Under Normal Physiological Conditions

Mice containing a global HspB2/HspB5 DKO have an increased heart to body weight ratio, including significantly increased left and right ventricle weights, during normal physiological or basal conditions [33]. There is no difference, however, in papillary muscle contractility [46]. In addition, the hearts of the DKO mice show increased Hsp60 expression and

HspB1 movement from the cytosolic to the cytoskeletal or nuclear regions of ventricular myocytes suggesting cardiac stress [47].

In contrast, cardiac-specific HspB2 deficiency does not alter heart and body weight ratios during basal conditions [32]. No effects on mitochondrial metabolism are detected under basal conditions, however, there is an elevated level of carnithine palmitoyltransferase 1 β (CPT-1β), a metabolic regulator involved in fatty acid oxidation, and decreased expression of isocitrate dehydrogenase 2 (IDH2), a mitochondrial metabolic regulator involved in glucose metabolism [32].

Knockout Effects Upon Ischemia/Reperfusion (I/R) Stress Conditions

Murine papillary muscles contract earlier and with greater strength during ischemia, followed by a reduction in contractile recovery during reperfusion [46]. When subject to I/R stress, HspB2/HspB5 DKO murine hearts display reduced myocardial contractile recovery and a blood pressure decline after induced contraction when compared to their wild type litter mates, while HspB2-deficient mice display decreases in systolic pressure, developed pressure, rate-pressure product and wall stress [33, 48]. Furthermore, there is a notable reduction in cardiac ATP production and recovery during reperfusion in the DKO and HspB2-deficient mouse [47] [33]. The diminished contractile recovery may be due to the inability of HspB2-deficient mice to efficiently utilize energy as there is a decreased coupling efficiency of the free energy of ATP hydrolysis and cardiac contractile performance [33]. In a cardiac-specific DKO mouse model, no detectable heart morphology abnormalities and no significant body weight alterations are present upon I/R insult [47]. Paradoxically, the DKO-deficiency decreases ischemic damage in mouse hearts, leading to decreased cardiac infract size, superoxide production, and creatine

kinase release [47]. The DKO-deficiency does, however, result in increased levels of apoptosis/necrosis, decreased levels of the antioxidant glutathione, increased mitochondrial permeability transition, lower levels of cytosolic $Ca2^{+}$ and higher levels of mitochondrial $Ca2^{+}$ in ventricular myocytes [49]. In addition, DKO mice display heightened cardiac Hsp60 protein levels [47] , suggesting greater difficulty in maintaining polypeptides in a folding-competent state. These results suggest that the DKO may provide the paradoxical protection by stimulating stress repair pathways that compensate for the deficiency.

Knockout Effects Upon Myocardial Mechanical or Chronic Pressure-Overload Stress Conditions

Although DKO protects from ischemia, there are defects seen in DKO mice during myocardial mechanical or chromic-overload stress conditions. Myocardial mechanical or pressure-overload stress induces cardiac hypertrophy, including an increased heart to body weight ratio, in fetal mice containing a global HspB2/HspB5-DKO [50]. No significant alterations in body weight are detected unless subject to chronic myocardial pressure-overload stress in which body weight decreases [50, 51]. The cardiac hypertrophic response worsens upon chronic pressure-overload with notably thickened cardiac walls, yet there is no chamber dilation [51]. This thickening may affect relaxation since both short-term and chronic pressure-overload stress in a global DKO mouse results in decreased myocardial and diastolic relaxation [50, 51]. Chronic stress also results in increased myocardial stiffness and abnormal cardiomyocyte cell volume, length, and profile area [51]. Pressure-overload stress in DKO mice results in increased NFAT transactivation, increased mRNA levels of ANF, β-MyHC, and skeletal actin, and decreased mRNA levels of α-MyHC, SERCA, and PLN [50]. This suggests an elevated immune

response and an attempt at contractile recovery. In mice with an HspB2-specific deficiency rather than DKO, hypertrophy is not detected in response to mechanical stress, indicating that HspB5 is responsible for preventing cardiac hypertrophy and not HspB2 [32].

Despite the lack of apparent myocardial abnormalities in the HspB2-specific KO, there are mitochondrial phenotypes under pressure-overload that are consistent with those observed under I/R stress. In a cardiac-specific HspB2 KO mouse, pressure-overload stress results in increased mRNA levels of Cox5b and MCAD, connoting an attempt to reinforce the respiration and mitochondrial fatty acid beta-oxidation pathways. However, pressure-overload stress in an HspB2 KO mouse results in lower mRNA levels of CPT-1β, a rate-controlling enzyme of the long-chain fatty acid beta-oxidation pathway. This is contrary to the effects of cardiac-specific HspB2 KO under basal conditions and suggests decreased mitochondrial fatty acid beta-oxidation during conditions of mechanical or pressure-overload stress [32]. Subsequently, depressed ATP production and fatty acid supported state 3 respiration rates are found in a cardiac-specific HspB2 KO mouse subject to pressure overload stress [32].

Anti-Apoptotic Properties

HspB2 dissuades apoptosis by inhibiting mitochondrial apoptotic events. Oshita et al. report that HspB2 over-expression in a human breast cancer cell line, cells that do not normally express HspB2, results in decreased apoptosis of this cell line [52]. Specifically, they found that HspB2 acts to inhibit the extrinsic apoptotic pathway induced by both TRAIL and TNF-α by suppressing TRAIL-induced caspases-3 activity and proteolytic processing of the apical procaspases-8 and -10. HspB2 also confers partial protection against apoptotic processes downstream of caspases-8, including the effects of tBid. These findings suggest that higher

expression of HspB2 negatively regulate mitochondrial and/or post-mitochondrial apoptotic events such as cytochrome c release and/or apoptosome-induced activation of caspases-9. In support of these findings, Oshita et al. found that mice containing human breast tumor cells expressing HspB2 are less sensitive to TRAIL treatment in comparison to mice treated with an empty vector, verifying the HspB2-dependent protection against TRAIL-induced apoptosis in vivo [52].

Table 1.1. The effects of HspB5/HspB2 or HspB2 deficiency in mouse hearts. Ŧ, Cardiac-Specific HspB2 KO; Ж, Global DKO with Global CryAB Over-expression; ψ, Fetal Murine.

CryAB/HpB2 DKO in Comparison to WT	HspB2 KO or Deficiency in Comparison to WT
Under Normal Physiological Conditions	
	Increased mRNA Levels of CPT-1 β Ŧ [32]
	Decreased mRNA Levels of IDH2 Ŧ [32]
Increased Heart Weight/Body Weight [33]	
Decreased Body Weight and Body Fat [45]	
Severe Spinal Curvature/Hunchback Phenotype [45]	
Severe Skeletal Muscle Degeneration [45]	
Upon Ischemia/Reperfusion Stress	
Decreased Contractile Recovery [46, 48]	Decreased Efficiency of ATP Hydrolysis Coupling to Cardiac Contractile Performance Ж [33]
Early and Greater Contraction of Papillary Muscles During Ischemia [46]	
Decreased Blood Pressure Upon Heart Contraction [33]	Decreased Systolic Pressure Ж [33]
Increased Apoptosis/Necrosis [48]	
Decreased Levels of Reduced Glutathione [48]	
Decreased Cytosolic Ca2+ Increase in Ventricular Myocytes [49]	
Increased Mitochondrial Up-take of Ca2+ in Ventricular Myocytes [49]	
Increased Mitochondrial Permeability Transition in Ventricular Myocytes [49]	
Increased HSP60 Protein Levels [47]	
Decreased Cardiac Infarct Size (by 35%) [47]	
Decreased Cardiac Superoxide Production [47]	
Decreased Cardiac Creatine Kinase Release [47]	
Decreaseed Cardiac ATP Production [47]	Decreased Cardiac ATP Recovery During Reperfusion Ж [33]
Upon Myocardial Mechanical or Pressure-Overload Stress	
Increased Cardiac Hypertrophy/ Increased Heart-Weight to Body-Weight Ratio ψ [50]	Unaffected Cardiac Hypertrophic Response Ŧ [32]
Defective Myocardial Relaxation ψ [50]	
Increased NFAT Transactivation ψ [50]	
Increased mRNA Levels of ANF, β-MyHC, and skeletal actin ψ [50]	Increased mRNA Levels of Cox5b and MCAD Ŧ [32]
Decreased mRNA Levels of α-MyHC, SERCA, and PLN ψ [50]	Decreased mRNA Levels of CPT-1β Ŧ [32]
	Decreased Fatty Acid Supported State 3 Respiration Rates, ADP Stimulated Ŧ [32]
	Decreased ATP Production Ŧ [32]
Upon Chronic Myocardial Pressure-Overload Stress	
Decreased Body Weight [51]	
Increased Cardiac Hypertrophy/ Thickened Cell Walls, but no Chamber Dilation [51]	
Decreased Diastolic Relaxation [51]	
Increased Myocardial Stiffness [51]	
Abnormal Cardiomyocyte Cell Phenotype [51]	

CONCLUSION

Small heat shock proteins play vital roles in maintaining cardiovascular function. The role of HspB2 in helping to prevent mitochondrial-related dysfunction and in maintaining proteostasis may be greater than previously considered. The consistently high energy demand of cardiac cells naturally results in greater risks for oxidative and reductive damage as the struggle to maintain REDOX balance and proteostasis continues. HspB2 may stabilize cardiac mitochondria in both basal and stress conditions. During normal physiological conditions, HspB2 loosely associates with the outer mitochondrial membrane in very low, nearly undetectable levels, where it associates with particular mitochondrial proteins of the myocardium [53]. During times of stress, HspB2 has been implicated in maintaining ATP production, ATP hydrolysis coupling to cardiac contractile performance, systolic pressure, and fatty acid supported state 3 respiration rates [32, 33]. Evidence clearly suggests that HspB2 plays an important role in stabilizing mitochondrial function of the myocardium, particularly during times of stress.

HspB2 also maintains cardiovascular function by protecting myofibrils and the actin cytoskeleton, preventing the erroneous aggregation of partially unfolded proteins, and inhibiting apoptosis in response to cardiac stress. While constitutively expressed in the myocardium, HspB2 expression is increased upon stretch stimulation and after birth [26, 28, 30]. As formerly noted, Ischemic and oxidative myocardial stress causes HspB2 to re-localize from the cytosol to the myofibril fraction or to the Z lines and intercalated discs where HspB2 may act to protect the actin cytoskeleton [30, 33, 34]. Nakagawa et al. showed that mouse fibroblast cells constitutively expressing HspB2 had a higher survival rate in comparison to wild type mouse fibroblasts when subjected to severe heat shock conditions of 44.5°C [31]. Increased temperatures may induce a

conformation change of HspB2, thereby resulting in increased levels of exposed hydrophobic regions that may interact with the increasingly exposed hydrophobic regions of denatured proteins [41, 42]. HspB2 may associate with misfolded proteins to prevent their aggregation during periods of stress, but may also cause proteins to continue to perform normal cellular functions by binding to and stabilizing such proteins [26, 41]. The mechanism by which this process may occur or by which HspB2 helps to maintain proteostasis is currently unknown, necessitating further research.

In addition to stabilizing mitochondria and myofibril structure, HspB2 may prevent or delay apoptosis in the heart, thereby providing longer time periods in which cellular damage may be corrected before cellular death ensues [52]. Of all of the sHSPs, HspB2 is the least studied and is the only one not directly associated with a human disease. The imperative role of HspB2 in cardiac maintenance strategies, both acting to prevent mitochondrial dysfunction and in maintaining proteostasis and cellular function, necessitates further exploration of its molecular function and therapeutic benefits.

CHAPTER TWO: Identification of the HspB2 Cardiac Interactome Reveals Unique Mitochondrial and Muscle Clients Involved in Myopathies and Neurodegenerative Disease

ABSTRACT

The first comprehensive HspB2 cardiac interactome is described herein as the first protein interaction network for any sHSP. Over two hundred proteins were identified as HspB2 binding partners, with significant overlap between yeast two-hybrid and copurification approaches. In addition to myofibril HspB2 binding partners, many mitochondrial binding partners were identified. The cardiac interactome identifies non-redundant roles for HspB2 in that the related sHSP, CryAB, bound only 40% of an interactome test subset. The HspB2 interactome predicts direct targets for studying HspB2 function, reveals non-redundant roles for CryAB and HspB2, provides a reference for studying overlapping and unique roles of the sHSP family, and predicts HspB2 association with diseases such as cardiomyopathy and Alzheimer's.

INTRODUCTION

Small heat shock proteins (sHsps) are molecular chaperones involved in protecting cells from a variety of stresses including normal cellular stress, extreme heat or cold, oxidative/reductive stress, and heavy metal-induced stress. Due to these critical roles, disruption in sHSP function is involved in the development of a wide range of diseases including ocular cataract disease and cardiomyopathy (for recent reviews see [54-64]). The sHSP family is characterized by their size (18-27 kDa) and conservation of a core α-crysallin domain flanked by highly variable sequence [65, 66]. Historically, sHSPs were thought to be redundant in function,

however sHsps vary in their cellular localization and tissue expression patterns suggesting they have differential roles [67].

Heat shock protein B2 (HSPB2), known originally as Mytotonic Dystrophy Protein Kinase Binding Protein (MKBP), is one of ten known sHSPs in the human genome [68]. HspB2 is encoded just upstream of a paralogous sHSP, αB-crystallin (CryAB or HspB5). HspB2 and CryAB were traditionally thought to share physiological and structural similarities as well as regulatory elements [69-75], however HspB2 is expressed at a lower level than CryAB, is not induced by heat shock, and is primarily found in cardiac and skeletal muscle whereas CryAB is ubiquitous [67]. Recent phenotypic data has identified differences in function as well.

The close proximity of CryAB and HspB2 hampered their individual characterization since original CryAB knock-out (KO) mice also removed regulatory regions necessary for HspB2 expression [76, 77]. Recently, the function of HspB2 was examined in pristine cardiac HspB2-deficient mice where HspB2-deficiency hampered state 3 respiration rates and ATP production during cardiac stress [78]. These results posit a role for HspB2 in mitochondrial function during cardiac stress and suggest that other sHSPs play somewhat redundant roles that are sufficient under basal conditions. However, the molecular mechanisms underlying HspB2 function, including protein clientele, are largely unknown.

The aim of this study was to identify molecular roles of HspB2 by determining the global cardiac protein interactome, the first comprehensive client search for any sHSP. Over 200 binding partners were identified for HspB2 through yeast two-hybrid and copurification analysis, a majority of which are mitochondrial. The HspB2 interactome also identifies binding partners for HspB2 that are not bound by CryAB, the first demonstration of non-redundant function

through clientele. Furthermore, all other sHSPs have been associated with diseases. The HspB2 interactome suggests that HspB2 may play a role in the development of myopathies and Alzheimer's disease.

METHODS

Yeast Two-Hybrid (Y2H) Screen and HspB2 Dependency Tests

Yeast harboring a cardiac cDNA Y2H prey library (Clontech) were mated to yeast harboring a full-length HspB2 bait plasmid using the standard Matchmaker mating protocol (Clontech). Over 22 million matings were performed, from which 10,000 colonies arose on Y2H selection plates (SD-Trp-Leu+ Aureobasidin) that were then patched to alternate Y2H selection plates (SD-Trp-Leu-His-Ade) for phenotype validation through alternate transcriptional reporters (HIS and ADE). The library plasmid inserts were identified for over 1500 colonies arising on the SD-Trp-Leu-His-Ade plates by colony PCR followed by sequencing and NCBI BLAST analysis. Any library plasmids hit more than once were then purified and transformed into yeast harboring the HSPB2-bait plasmid as well as yeast harboring the empty bait plasmid to test for HSPB2 dependency.

HSPB2cTG Mouse Line

Human cDNA of HSPB2 was amplified and inserted after the a-myosin heavy chain (MHC) promoter1 (Figure 2A)(Gulick J, Hewett TE, Klevitsky R, Buck SH, Moss RL, Robbins J. Transgenic remodeling of the regulatory myosin light chains in the mammalian heart. Circ Res. 1997; 80:655-664.). Transgenic (TG) mice were generated and maintained in a mixed genetic background with C57Bl/6J and 129S6 contributions. The HSPB2cTG mice were genotyped by

PCR with following primers: forward aggcagggaagtggtggtgtagg and reverse ggccttctccgaagcgctgc.

Mitochondrial Coaffinity Proteomics Experiments

Mitochondrial HspB2 was immunopurified from mice harboring either transgenic (TG) HSPB2 or an HSPB2 knockout (KO). In each group, mitochondria were combined from four mouse hearts, lysed in 0.1% NP-40 homogenization buffer and 2 mg was incubated with anti-HspB2 antibodies. The IP eluates were then fractionated on SDS-PAGE, excised and analyzed by LC-MS/MS. Samples had one biological replicate and two technical replicates. Technical replicates showed greater than 90% overlap. The raw data were analyzed by BioWorks (ThermoFisher Scientific, version 3.3.1 SP1) and proteins were identified using SEQUEST (ThermoFisher Scientific, version 3.3.1) and Scaffold (Proteome Software, version 3.3.3). At least 2 peptides and 99.0% protein confidence were required for protein algorithms; the global false discovery rate was 0.1%.

Bioinformatics/Network Analysis

Cytoscape version 2.8.1 [79] was used to retrieve previously identified protein-protein interactions from the Reactome, IntAct, HPRD, HumanCyc, MINT, the MSKCC Cancer Cell Map, and the NCI/Nature Pathway Interaction databases for each of the HspB2 binding partners and to map them into a single merged network. Gene Ontology analysis (Cytoscape ClueGO plugin[80]) for the resulting networks was used to reveal function and cellular localization. The Online Mendelian Inheritance in Man (OMIM) database was used to search for any known disease association for each of the HspB2 binding partners.

HspB2 and CryAB Binding Partner Comparison

Yeast two-hybrid (Y2H) assays for direct binding between HspB2 and 15 binding partners compared with direct binding to the related sHSP, CryAB. Y2H prey plasmids containing the indicated genes were transformed into Y2HGold (Contech) containing bait plasmids with either HspB2, CryAB, or an empty vector. Overnight yeast cultures were grown for 48 hours in SD-Trp-Leu to select for plasmids, then serially diluted and plated on SD-Trp-Leu-His-Ade plates to select for protein-protein interaction.

RESULTS

An Unbiased Yeast Two-hybrid (Y2H) Screen for HspB2 Substrates Identifies Novel Cardiac Clients

In order to identify the molecular pathways of cardiac HspB2 function we conducted an unbiased, large-scale Y2H screen for protein-protein interaction partners. A human heart cDNA yeast two-hybrid prey library (Clontech) was mated to yeast containing an HspB2 bait plasmid. From over 25 million matings, approximately 10,000 putative interactions were detected of which 1,883 prey plasmids were sequenced to identify the interacting partner. Only one of every ~2,000 matings resulted in a positive Y2H interaction suggesting specificity in target for HspB2. Sequencing revealed a large number of interacting partners as expected for a molecular chaperone (558 unique hits).

An advantage of the Y2H method is its high sensitivity, which can also result in a high false positive rate ([81-83]). In order to confirm the protein-protein interactions identified in the screen, plasmids encoding 72 of the binding partners were purified from yeast and reintroduced

into naïve yeast harboring either the empty bait plasmid or the HspB2 bait plasmid. These binding partners were grouped depending on if they were retrieved multiple times (Table 2.1) or only once (Table 2.4) in the Y2H screen. Remarkably, 81% of these multi-hit library plasmids showed a positive Y2H result only when HspB2 was present, 11% were false positives (they grew with either HspB2 or the empty bait plasmid), and 8% were true negatives (they did not grow when retransformed). In contrast, 51% of the single hit binding partners were HspB2 dependent, with a 12% false positive rate and a 37% true negative rate. Thus, our multi-hit list with an 81% validation rate is the most reliable and was used in all further analysis.

Of the proteins found to interact with HspB2, 33% were found to primarily localize to the cytoplasm in the cell, while 19% localize primarily to the mitochondria and 13% to the nucleus (Figure 2.1A). HspB2 has previously been reported to relocate from the cytosol to the mitochondria and nucleus during events of cellular stress [31], lending support to our findings. Many of the interacting partners are muscle fiber-related proteins (19%), consistent with the previously reported role of HspB2 in muscle fiber maintenance ([68, 84-88]) (Figure 2.1B). In addition, 19% of the binding partners are mitochondrial proteins including many respiratory chain proteins, supporting the role of HspB2 in ATP production [76, 78, 84].

These data represents the first global interactome for any sHSP. It not only provides insight into the possible clientele of HspB2, but also serves as a resource for uncovering differential roles of the sHSPs. It is worth noting, however, that HspB2 binding partners could be undetected in our screen due to underrepresentation in the cardiac cDNA library, misfolding of the chimeric Y2H protein, or the absence of accessory proteins/factors or proper localization. Thus, multiple complementary approaches are recommended when obtaining protein interactomes.

A.

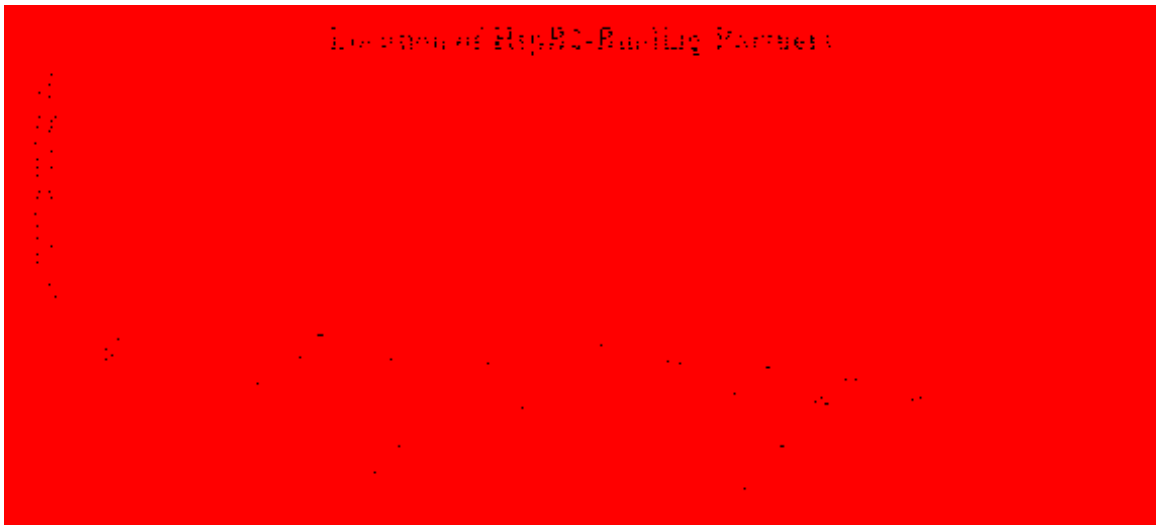

B.

Figure 2.1. Analysis of the HspB2 Y2H cardiac interactome reveals key roles in mitochondrial function and myofibril maintenance. Bar graphs summarizing the Y2H screen indicating localization (**A**) and function (**B**). Function was assigned by basic description on Genecards (Stelzer et al., 2011), UniProt [89, 90] or literature searches when necessary. Location was assigned by UniProt (Magrane and Consortium, 2011).

Table 2.1- Putative HspB2 binding partners retrieved from the Y2H screen more than once.

Myofibril or Cytoskeleton Structure/Regulation					
Actin binding LIM protein 1	O14639	ABLIM1	Cytoskeleton	2	ND
Actin, alpha 1, skeletal muscle	P68133	ACTA1	Cytoplasm	8	Yes
Actin, beta	P60709	ACTB	Cytoplasm	2	ND
Actin, alpha, cardiac muscle 1	P68032	ACTC1	Cytoplasm	37	ND
Actin, gamma 1	P63261	ACTG1	Cytoplasm	5	ND
Capping protein (actin filament) muscle Z-line, alpha2	P47755	CAPZA2	Cytoskeleton	3	ND
Cardiomyopathy associated 5	Q8N3K9	CMYA5	Cytoskeleton	4	Yes
Biglycan	P21810	BGN	Extracellular	2	ND
Dynactin 1 (	Q14203	DCTN1	Cytoskeleton	3	Yes
Enolase 3 (beta, muscle) (	P13929	ENO3	Extracellular	7	Yes
Filamin C, gamma (	Q14315	FLNC	Cytoplasm	2	ND
Myosin binding protein C, cardiac	Q14896	MYBPC3	Cytoplasm	11	Yes
Myosin, heavy chain 6, cardiac muscle, alpha	P13533	MYH6	Cytoplasm	3	Yes
Myosin, heavy chain 7, cardiac muscle, beta	A5YM51	MYH7	Extracellular	14	Yes
Myosin, light chain 2, regulatory, cardiac, slow	P10916	MYL2	Cytoplasm	5	Yes
Myosin, light chain 3, alkali; ventricular, skeletal, slow	P08590	MYL3	Cytoplasm	2	Yes
Myomesin (M-protein) 2	P54296	MYOM2	Cytoplasm	6	Yes
Palladin	Q8WX93	PALLD	Cytoplasm	2	ND
Phosphatidic acid phosphatase type 2 domain containing 3	Q8NBV4	PPAPDC3	Plasma Membrane	2	ND
Ryanodine receptor 2 (cardiac)	Q92736	RYR2	Cytoplasm	3	ND
Synaptopodin	A7MD96	SYNPO	Cytoskeleton	2	ND
Titin-cap (telethonin)	O15273	TCAP	Cytoplasm	6	ND
Troponin I type 3	Q6FGX2	TNNI3	Cytoplasm	5	Yes
WD repeat domain 1	O75083	WDR1	Cytoplasm	3	ND
Xin actin-binding repeat containing 1	Q702N8	XIRP1	Plasma Membrane	2	ND
Fermentation/Respiration					
Acetyl-CoA acyltransferase 2	P42765	ACAA2	Mitochondria	5	Yes
Aldehyde dehydrogenase 2 family (mitochondrial)	P05091	ALDH2	Mitochondria	2	ND
Aldolase A, fructose-biphosphate	P04075	ALDOA	Cytoplasm	15	Yes
ATP synthase, H+ transporting F1 complex, alpha subunit 1,	P25705	ATP5A1	Mitochondria	11	Yes
Cytochrome c oxidase subunit IV isoform 1	P13073	COX4I1	Mitochondria	2	ND
Cytochrome C oxidase subunit Vic	P09669	COX6C	Mitochondria	14	ND
Cytochrome C oxidase subunit Viib	P24311	COX7B	Mitochondria	3	Yes
Cytochrome P450, family 1, subfamily B, polypeptide 1	Q16678	CYP1B1	ER	4	ND
Enolase 1	P06733	ENO1	Cytoplasm	4	ND
Electron-transfer-flavoprotein, alpha polypeptide	P13804	ETFA	Mitochondria	15	Yes
Glyceraldehyde-3-phosphate dehydrogenase	P04406	GAPDH	Cytoplasm	19	Yes
Hydroxyacyl-CoA dehydrogenase/3-ketoacyl-CoA thiolase	P55084	HADHB	Mitochondria	5	Yes
Isocitrate dehydrogenase 2 (NADP+), mitochondrial	P48735	IDH2	Mitochondria	3	Yes
Methylcrotonoyl-CoA carboxylase 2	Q9HCC0	MCCC2	Mitochondria	2	ND
Malate dehydrogenase 1, NAD (soluble)	P40925	MDH1	Cytoplasm	2	ND
Cytochrome c oxidase III	P00414	MT-CO3	Mitochondria	2	ND
Mitochondrial NADH dehydrogenase subunit 1	P03886	MT-ND1	Mitochondria	118	ND

Mitochondrial NADH dehydrogenase subunit 2	P03891	MT-ND2	Mitochondria	9	ND
Mitochondrial NADH dehydrogenase 4	P03905	MT-ND4	Mitochondria	8	ND
NADH dehydrogenase (ubiquinone) 1 alpha subcomplex 6	P56556	NDUFA6	Mitochondria	2	Yes
NADH dehydrogenase (ubiquinone) 1 alpha subcomplex, 13	Q9P0J0	NDUFA13	Mitochondria	2	ND
Oxoglutarate (alpha-ketoglutarate) dehydrogenase	A2VCT2	OGDH	Mitochondria	2	Yes
Phosphoglucomutase 1	P36871	PGM1	Cytoplasm	2	ND
Succinate dehydrogenase complex, subunit A, flavoprotein	D6RFM5	SDHA	Mitochondria	5	Yes
Similar to cytochrome c oxidase II	O43819	SCO2	Mitochondria	2	ND
Signal Transduction					
Ankyrin repeat & GTPase domain Arf GTPase activating protein 11	Q8TF27	AGAP11		2	ND
Axin 1	O15169	AXIN1	Nucleus	2	ND
DAZ associated protein 2	Q15038	DAZAP2	Cytoplasm	17	Yes
Dysbindin domain containing 2	Q9BQY9	DBNDD2	Cytoplasm	4	Yes
DNA-damage-inducible transcript 4	Q9NX09	DDIT4	Cytoplasm	2	ND
Dual-specificity Y-phosphorylation regulated kinase 1A	Q13627	DYRK1A	Nucleus	2	Yes
Dual specific phosphatase 1	P28562	DUSP1	Nucleus	2	ND
Four and a half LIM domains 2	Q14192	FHL2	Nucleus	10	Yes
G protein-coupled receptor 146	Q96CH1	GPR146	Plasma Membrane	2	Yes
Low density lipoprotein receptor-related protein 10	Q7Z4F1	LRP10	Plasma Membrane	2	ND
Myozenin 2	Q9NPC6	MYOZ2	Cytoplasm	2	ND
Parvin, alpha	Q9NVD7	PARVA	Plasma Membrane	2	ND
Plexin-A4	Q9HCM2	PLXNA4	Extracellular	2	ND
Prosaposin	Q5BJH1	PSAP	Lysosome	14	ND
Small G protein signaling modulator 2	O43147	SGSM2		2	ND
SH3 domain binding glutamic acid-rich protein	P55822	SH3BGR	Cytoplasm	3	ND
Syntrophin, alpha 1 (dystrophin-associated protein A1)	Q13424	SNTA1	Cytoplasm	2	ND
TNFAIP3 interacting protein 1	Q15025	TNIP1	Cytoplasm	2	ND
Zinc finger protein 335	Q8IW09	ZNF335	Nucleus	2	Yes
Zyxin	Q15942	ZYX	Cytoplasm	2	ND
Protein Biosynthesis and Processing					
Brain expressed X-linked 4	Q9NWD9	BEX4	Cytoplasm	2	ND
Eukaryotic translation elongation factor 1 alpha 1	P68104	EEF1A1	Cytoplasm	13	Yes
Eukaryotic translation elongation factor 2	Q6PK56	EEF2	Cytoplasm	2	ND
Eukaryotic translation initiation factor 1B	O60739	EIF1B	Nucleus	2	ND
Eukaryotic translation initiation factor 4A2	Q14240	EIF4A2	Cytoplasm	3	ND
Glycyl-tRNA synthetase	P41250	GARS	Cytoplasm	2	ND
Asparaginyl-tRNA synthetase	O43776	NARS	Cytoplasm	2	ND
NHP2 non-histone chromosome protein 2-like 1	P55769	NHP2L1	Nucleus	2	ND
RNA binding protein fox-1 homolog 2 isoform 6	O43251	RBFOX2	Nucleus	2	Yes
Ribosomal protein L11	P62913	RPL11	Ribosome	10	Yes
Ribosomal protein L36a	J3KQN4	RPL36A	Cytoplasm	13	Yes
Ribosomal protein L35a-like	Q969Q0	RPL36AL	Ribosome	2	ND
Ribosomal protein S11	P62280	RPS11	Ribosome	4	ND
THUMP domain containing 2	Q9BTF0	THUMPD2		2	ND

Transport					
ATP-binding cassette, subfamily C, member 9	O60706	ABCC9	Plasma Membrane	2	ND
ATP-binding cassette, sub-family D, member 4	O14678	ABCD4	Peroxisome	2	ND
ATPase, H+ transporting, V1 subunit E1	Q53Y06	ATP6V1E1	Lysosome	2	ND
Myoglobin		MB	Cytoplasm	3	ND
Nucleoporin 62kDa	P37198	NUP62	Nucleus	2	ND
Protein phosphatase, IK	Q8N3J5	PPM1K	Mitochondria	2	ND
Stromal cell-derived factor 2	Q99470	SDF2	Extracellular	2	ND
Solute carrier family 2, member 1	P11166	SLC2A1	Plasma Membrane	3	ND
Solute carrier family 25, member 3	Q00325	SLC25A3	Mitochondria	2	ND
Solute carrier family 25 , member 4	P12235	SLC25A4	Mitochondria	3	Yes
Transportin 2	Q05D48	TNPO2	Nucleus	6	ND
Protein Degradation					
Alpha-2-macroglobulin	P01023	A2M	Extracellular	3	ND
Cathepsin B	P07858	CTSB	Lysosome	4	ND
Cathepsin D	P07339	CTSD	Lysosome	4	Yes
Proteaseome (prosome, macropain) subunit, beta type, 1	P02144	PSMB1	Cytoplasm	2	ND
Ubiquitin speicifc peptidase 28	Q6NZX9	USP28	Nucleus	3	ND
Ubiquitin specific peptidase 7 (herpes virus-associated)	Q93009	USP7	Nucleus	2	ND
Nucleotide Metabolism					
Creatine kinase, brain	P12277	CKB	Cytoplasm	2	ND
Creatine kinase, muscle	P06732	CKM	Cytoplasm	3	ND
Guanylate kinase 1	Q96IN2	GUK1	Cytoplasm	3	Yes
Homeodomain interacting protein kinase 2	Q9H2X6	HIPK2	Nucleus	2	ND
TatD DNase domain containing 1	Q6P1N9	TATDN1	Nucleus	2	ND
Immune					
Beta-2 microglobulin		B2M	Extracellular	8	Yes
Complement component 1, q subcomponent, A chain	P02745	C1QA	Extracellular	2	ND
Cyclin D-type binding protein 1	O95273	CCNDBP1	Extracellular	2	Yes
CD14 molecule	P08571	CD14	Extracellular	3	ND
Thymocyte selection associated family member 2	Q5TEJ8	THEMIS2		2	ND
Cell Adhesion					
Lectin, galactoside-binding, soluble, 1	P09382	LGALS1	Extracellular	9	Yes
Neural cell adhesion molecule 1 isoform 5 precursor	P13591	NCAM1	Plasma Membrane	2	ND
Plakophilin 2	Q99959	PKP2	Nucleus	3	ND
Transmembrane protein 8A	Q9HCN3	TMEM8A	Plasma Membrane	2	ND
Osmoregulation					
ATPase, Na+/K+ transporting, beta 1	Q6LEU2	ATP1B1	Plasma Membrane	2	ND
Sodium channel voltage-gated, type I, beta	Q07699	SCN1B	Plasma Membrane	3	ND
Uncoupling protein 2	P55851	UCP2	Mitochondria	2	ND
Small Molecule Biosynthesis					
N-acylsphingosine amidohydrolase (acid ceramidase) 1	Q13510	ASAH1	Lysosome	2	ND
Methylmalonic aciduria (cobalamin deficiency) cb1D type	Q9H3L0	MMADHC	Mitochondria	4	Yes

Oxidoreductive Stress					
Glutathione peroxidase 3 (plasma)	P22352	GPX3	Extracellular	2	Yes
Thioredoxin interacting protein	Q9H3M7	TXNIP	Cytoplasm	6	ND
Chaperone					
Crystallin, alpha B	P02511	CRYAB	Nucleus	34	Yes
Replication/Recombination					
PAP associated domain containing 5	Q8NDF8	PAPD5	Nucleus	2	ND
Intracellular Trafficking					
Translocation protein SEC62	Q99442	SEC62	ER	3	ND
Iron and Copper Homeostasis					
Ferritin, light polypeptide	P02792	FTL	Cytoplasm	2	Yes
Uncharacterized					
ATP5S-like	Q9NW81	ATP5SL		2	Yes
Cysteine/tyrosine-rich 1	Q96J86	CYYR1	Plasma Membrane	2	ND
Dynactin 6	O00399	DCTN6	Mitochondria	3	ND
Four and a half LIM domains 1	Q13642	FHL1	Cytoplasm	2	ND
FERM domain-containing protein 5 isoform 2	Q7Z6J6	FRMD5	Plasma Membrane	2	ND
Myeloid leukemia factor 2	Q15773	MLF2	Nucleus	2	ND
MT-RNR2-like 2	P0CJ69	MTRNR2L2	Cytoplasm	3	ND
Nucleotidase domain containing 2	Q9H857	NT5DC2		2	ND
5' Upstream region of mito-encoded Olfactory receptor			Mitochondria	503	Yes

The data in this table contains the following information sequentially: protein name, UniProt protein accession number, gene symbol, cellular localization reported on HPRD or Genecards, and the number of times it was retrieved from the screen and the results of Hspb2 dependency tests where applicable. The hits are those retrieved more than once from the Y2H screen (143 hits) and are functionally categorized by their description on UniProt and/or Genecards. ND is not determined. See supplementary Table S1 for a complete list of putative HspB2 binding partners retrieved from the Y2H screen only once.

Validating the Y2H HspB2 Interactome Through Coaffinity Proteomics.

A widespread proteomics approach that complements Y2H analysis well is copurification followed by quantitative mass spectroscopy [91, 92]. An advantage of this approach is the ability to detect native proteins in their native environment. HspB2 was immunopurified from cardiac muscle mitochondria derived from mice harboring either transgenic (TG) HSPB2 or an HSPB2 knockout (KO). Heart-specific HSPB2cTG mice were generated by over-expressing human HSPB2 from a-myosin heavy chain (a-MyHC) promoter.

Copurified proteins were run on SDS-PAGE for fractionation and then identified by quantitative LC/MS/MS. HspB2 was identified in the TG HspB2 samples, but not in the WT or KO samples, presumably due to low expression in WT tissue. Although 92% of proteins found in the HspB2 KO group were also in the HspB2 TG group, the HspB2 TG samples harbored 67 proteins not detected in the HspB2 control group (Fig. 2.2A; Table 2.2). In addition, these 67 proteins were enriched in membrane bound proteins (63%) functioning in oxidative phosphorylation, transport and signaling when compared to the proteins in the HspB2 KO samples (data not shown) consistent with HspB2 associating with the outer membrane of mitochondria [93] and functioning in ATP production during cardiac stress [78, 84].

A.

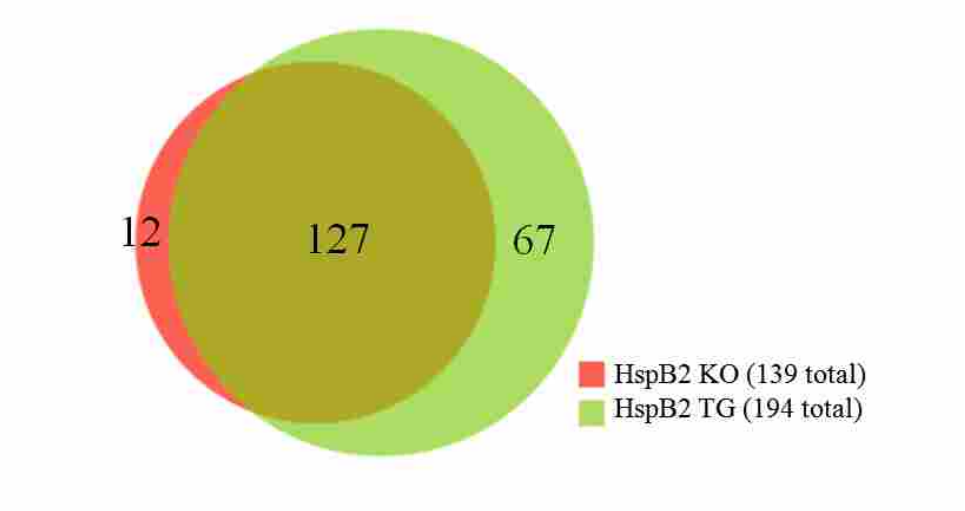

B.

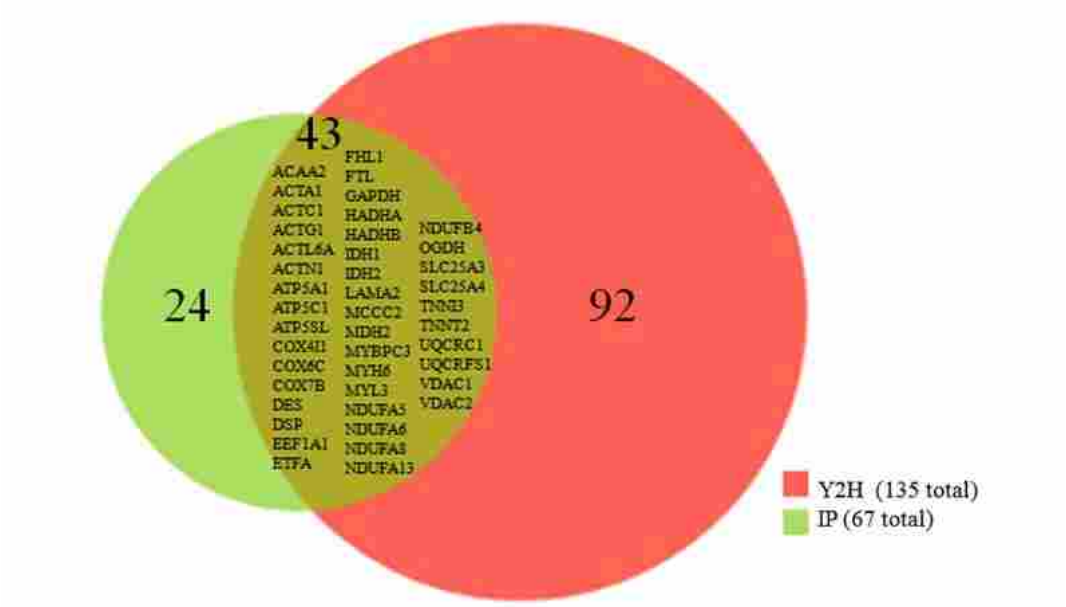

Figure 2.2. Analysis of the HspB2 mitochondrial copurification interactome reveals remarkable agreement with the Y2H interactome. (**A**) Unique proteins identified in HSPB2 TG immunoprecipitation verses the HSPB2 KO control. (**B**) A Venn diagram of the putative HspB2 binding proteins from Y2H and mitochondrial proteomics and their overlap. The hits that overlapped included ACAA2, ACTA1, ACTC1, ACTG1, ACTL6A, ACTN1, ATP5A1, ATP5C1, ATP5SL, COX4I1, COX6C, COX7B, DES, DSP, EEF1A1, ETFA, FHL1, FTL, GAPDH, HADHA, HADHB, IDH1, IDH2, LAMA2, MCCC2, MDH2, MYBPC3, MYH6, MYL3, NDUFA5, NDUFA6, NDUFA8, NDUFA13, NDUFB4, OGDH, SLC25A3, SLC25A4, TNNI3, TNNT2, UQCRC1, UQCRFS1, VDAC1, VDAC2.

Table 2.2. Unique proteins identified from the HSPB2 TG group when compared to the HSPB2 KO group.

Oxidative Phosphorylation					
NADH-ubiquinone oxidoreductase chain 1	P03888	mt-nd1	36,012	318	Mitochondrial Inner Membrane
NADH-ubiquinone oxidoreductase chain 4	P03911	mt-nd4	51,869	459	Mitochondrial Inner Membrane
NADH-ubiquinone oxidoreductase chain 5	P03921	mt-nd5	68,441	607	Mitochondrial Inner Membrane
NADH dehydrogenase [ubiquinone] 1 alpha subcomplex subunit 11	Q9D8B4	Ndufa11	14,965	141	Mitochondrial Inner Membrane
NADH dehydrogenase [ubiquinone] 1 beta subcomplex, 11	B1AV40	Ndufb11	17,426	151	Mitochondrion
NADH dehydrogenase [ubiquinone] 1 beta subcomplex subunit 3	Q9CQZ6	Ndufb3	11,674	104	Mitochondrial Inner Membrane
NADH dehydrogenase [ubiquinone] 1 beta subcomplex, 6	A2AP31	Ndufb6	15,498	128	Mitochondrial Inner Membrane
NADH dehydrogenase [ubiquinone] 1 beta subcomplex subunit 8, mitochondrial	Q9D6J5	Ndufb8	21,858	186	Mitochondrial Inner Membrane
NADH dehydrogenase [ubiquinone] 1 beta subcomplex subunit 9	Q9CQJ8	Ndufb9	21,966	179	Mitochondrial Inner Membrane
NADH dehydrogenase [ubiquinone] 1 subunit C2	Q9CQ54	Ndufc2	14,146	120	Mitochondrial Inner Membrane
NADH dehydrogenase (Ubiquinone) 1 beta subcomplex, 5, isoform CRAe	D3Z568	Ndufb5	14,038	119	Mitochondrial Inner Membrane
Ubiquinol-cytochrome c reductase hinge protein	B1ASG5	Uqcrh	10,417	89	Mitochondrial Inner Membrane
Cytochrome b-c1 complex subunit 8	Q9CQ69	Uqcrq	9,751	82	Mitochondrial Inner Membrane
Cytochrome c oxidase subunit 7A-related protein, mitochondrial	E9PZS8	Cox7a2l	14,913	134	Mitochondrial Inner Membrane
ATP synthase subunit e, mitochondrial	Q06185	Atp5i	8,218	71	Mitochondrial Inner Membrane
ATP synthase subunit g, mitochondrial	Q9CPQ8	Atp5l	11,407	103	Mitochondrial Inner Membrane
Transport					
Apolipoprotein O	B1ASQ2	Apoo	22,587	198	Apolipoprotein O
Apolipoprotein O-like	B1AV13	Apool	29,244	265	Mitochondrial Inner Membrane
Brain protein 44	Q9D023	Brp44	14,269	127	Mitochondrial Inner Membrane
Mitochondrial carrier homolog 2	A2AFW6	Mtch2	32,328	294	Mitochondrial Inner Membrane
Metaxin 2	A2AT31	Mtx2	29,740	263	Mitochondrial Outer Membrane
Sorting and assembly machinery component 50 homolog	Q8BGH2	Samm50	51,847	469	Mitochondrial Outer Membrane
Calcium-binding mitochondrial carrier protein Aralar1	Q8BH59	Aralar1, Slc25a12	74,554	677	Mitochondrial Inner Membrane
Mitochondrial carnitine/acylcarnitine carrier protein	Q9Z2Z6	Slc25a20	33,010	301	Mitochondrial Inner Membrane
AP-3 complex subunit delta-1	O54774	Ap3d1	135,081	1199	Membrane

ADP/ATP translocase 2	P51881	Slc25a5, Ant2	32,915	298	Mitochondrial Inner Membrane
Nascent polypeptide-associated complex subunit alpha, muscle-specific form	P70670	Naca	220,499	2187	Cytoplasm, Nucleus
Solute carrier family 25 member 42	Q8R0Y8	Slc25a42	35,241	318	Mitochondrial Inner Membrane
Translocase of inner mitochondrial membrane domain containing 1	Q8BUY5	Timmdc1	31,774	285	Mitochondrial Inner Membrane
Signaling					
Platelet glycoprotein 4	Q08857	Cd36	52,681	472	Golgi Apparatus
CDGSH iron-sulfur domain-containing protein 1	Q91WS0	Cisd1	12,079	108	Mitochondrial Outer Membrane
Crip2 protein	Q4FJU3	Crip2	22,709	208	Cell Cortex
Heat shock protein beta-2	E9QKE3	Hspb2	20,357	182	
Ras-related protein Rab-7a	P51150	Rab7a Rab7	23,472	207	Endosome, Lysosome
Isoform 2 of Perilipin-4	O88492	Plin4	139,415	1403	Cytoplasm, Cell Membrane
Complement component 1 Q subcomponent-binding protein, mitochondrial	O35658	C1qbp	31,013	278	Mitochondrial Matrix
EH-domain containing 4	Q3TM70	Ehd4	61,481	541	ER, Plasma Membrane
Heat shock cognate 71 kDa protein	P63017	Hspa8	70,871	646	Cytoplasm
Novel protein GN=Mtfp1	Q5SQ26	Mtfp1	18,314	166	Mitochondria
Structure					
Alpha actinin 1a	A1BN54	Actn1	102,706	887	Z disc
Uncharacterized protein GN=Vim	E9PZV5	Vim	52,185	453	Cytoplasm, Intermediate Filament
Spectrin alpha 2	A3KGU5	Spna2	282,895	2457	Cytoskeleton
Isoform 2 of Spectrin beta chain, brain 1	Q62261	Spnb2	274,223	2363	Cytoskeleton
Perlecan (Heparan sulfate proteoglycan 2)	B1B0C7	Hspg2	469,023	4735	Basal lamina
Troponin C, slow skeletal and cardiac muscles	P19123	Tnnc1	18,421	161	Cytoskeleton
Metabolism					
Protein Acad12	D3Z2B3	Acad12	41,332	373	Mitochondrion
Amine oxidase [flavin-containing] B	Q8BW75	Maob	58,541	520	Mitochondrial Outer Membrane
Methylcrotonoyl-CoA carboxylase subunit alpha, mitochondrial	Q99MR8	Mccc1	79,327	717	Mitochondrial Inner Membrane /Matrix
Methylcrotonoyl-Coenzyme A carboxylase 2 (Beta)	B2RUK5	Mccc2	61,362	563	Mitochondrion
NAD(P) transhydrogenase, mitochondrial	Q61941	Nnt	113,823	1,086	Mitochondrial Inner Membrane
Ferrochelatase (EC 4.99.1.1)	F7CAB4	Fech	44,667	399	Mitochondrial Inner Membrane
The Citric Acid Cycle					
Dihydrolipoyl dehydrogenase, mitochondrial	O08749	Dld	54,254	509	Mitochondrial Matrix
Uncharacterized protein GN=Ogdhl	E9Q7L0	Ogdh1	116,584	1,029	Mitochondrion

Isoform 2 of Dihydrolipoyllysine-residue succinyltransferase component of 2-oxoglutarate dehydrogenase complex, mitochondrial	Q9D2G2	Dlst	22,212	454	Mitochondrion, Nucleus
2-oxoglutarate dehydrogenase, mitochondrial	E9Q1C6	Ogdh	117,741	214	Mitochondrion Matrix
Cell Adhesion					
Laminin subunit alpha-2	E9Q965	Lama2	342,761	3,105	Sarcolemma
Nidogen-1	P10493	Nid1	136,519	1,245	Extracellular Matrix
Laminin subunit gamma-1	P02468	Lamc1	177,298	1607	Sarcolemma
Vinculin	Q64727	Vcl	116,717	1066	Cytoskeleton
Lipid Metabolism					
Carnitine O-palmitoyltransferase 1, muscle isoform	Q924X2	Cpt1b	88,202	772	Mitochondrial Outer Membrane
Carnitine palmitoyltransferase 2	A2A8E7	Cpt2	24,889	223	Mitochondrial Inner Membrane
Carnitine O-acetyltransferase	P47934	Crat	70,823	626	ER, Mitochondrial Inner Membrane, Peroxisome
DNA/RNA/Protein Biosynthesis					
39S ribosomal protein L12, mitochondrial	Q9DB15	Mrpl12	21,691	201	Mitochondrion
Prohibitin	P67778	Phb	29,803	272	Mitochondrial Inner Membrane
Apoptosis					
Apoptosis-inducing factor, mitochondrion-associated 1	B1AU24	Aifm1	66,748	612	Mitochondrial Intermembrane Space/Outer Membrane
Dynamin-like 120 kDa protein, mitochondrial	E0CXD1	Opa1	78,918	692	Mitochondrial Inner Membrane
Amino Acid Metabolism					
Methylglutaconyl-CoA hydratase, mitochondrial (Fragment)	F6R307	Auh	22,898	219	Mitochondrion
Unknown					
ES1 protein homolog, mitochondrial	Q9D172	D10Jhu81e	28,072	266	Mitochondrion

This table lists information on all 67 uniquely identified proteins from the HSPB2 TG samples compared with the HSPB2 KO samples by quantitative mass spectroscopy. It contains the following information sequentially: protein name, Uniprot protein accession number, gene symbol, molecular weight (MW), protein length (# of amino acids), and cellular localization from HPRD or GenecardsThe proteins are those are functionally categorized by their description on UniProt and/or Genecards.

The Y2H and Copurificaton HspB2 Mitochondrial Interactomes Display 80% Overlap.

Results from the global cardiac Y2H and the cardiac mitochondrial copurification screens are in remarkable agreement with over 80% of the Y2H mitochondrial hits identified by copurification (Figure 2.2B). This may in part be due to the abundance of mitochondria in cardiac tissue, yet the agreement is remarkable when considering the total mitochondrial proteome. Over 1,000 mitochondrial proteins are estimated in studies of both human [94] and rat [95] cardiac tissue. In addition, a majority of the overlapping mitochondrial proteins from both screens are known binding partners as shown by Cytoscape network analysis (Figure 2.3A). Amid the 73 mitochondrial protein partners of HspB2, 47 were already known to interact directly with at least one other mitochondrial protein with 100 total interactions identified in this protein interaction network.

A.

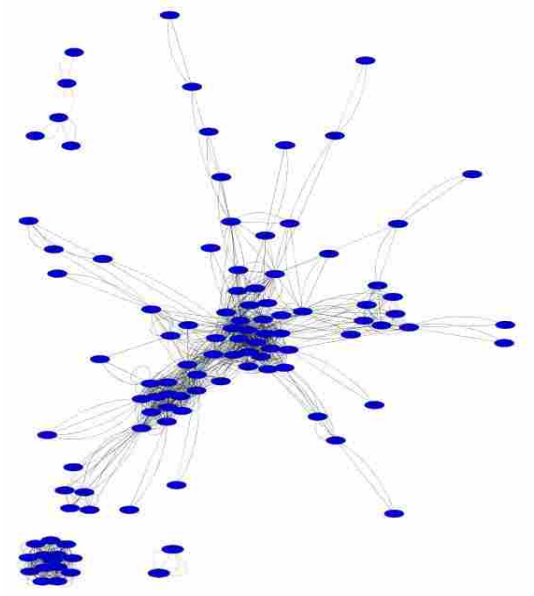

B.

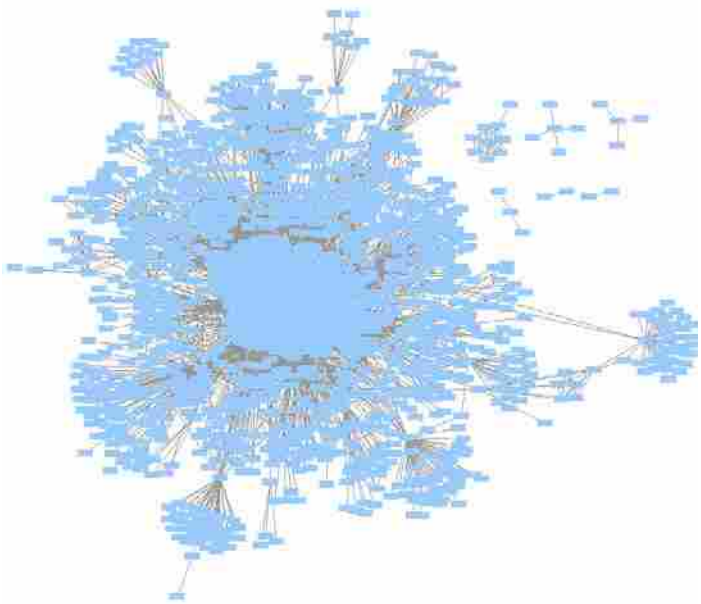

C.

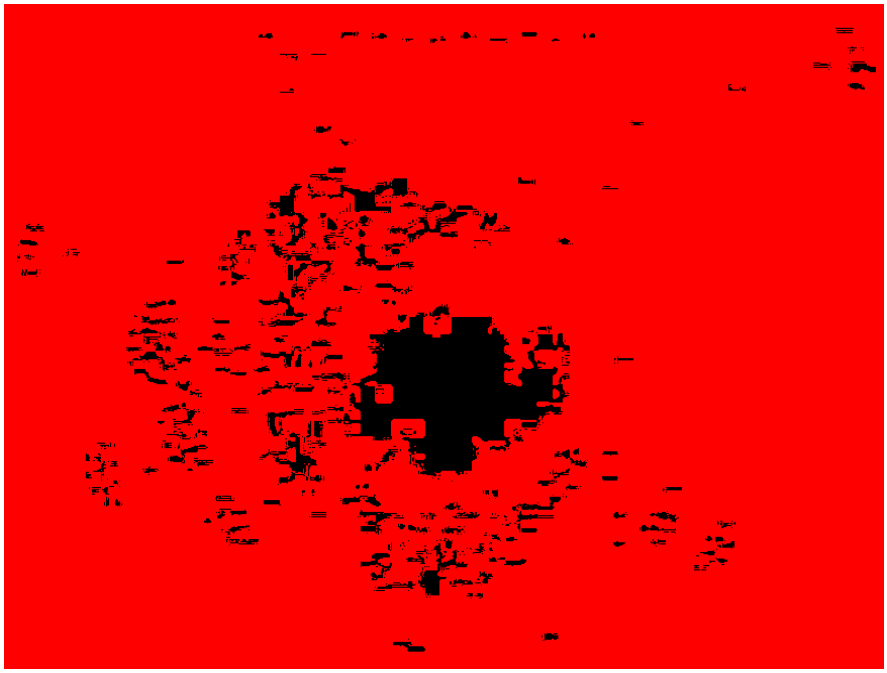

D.

E.

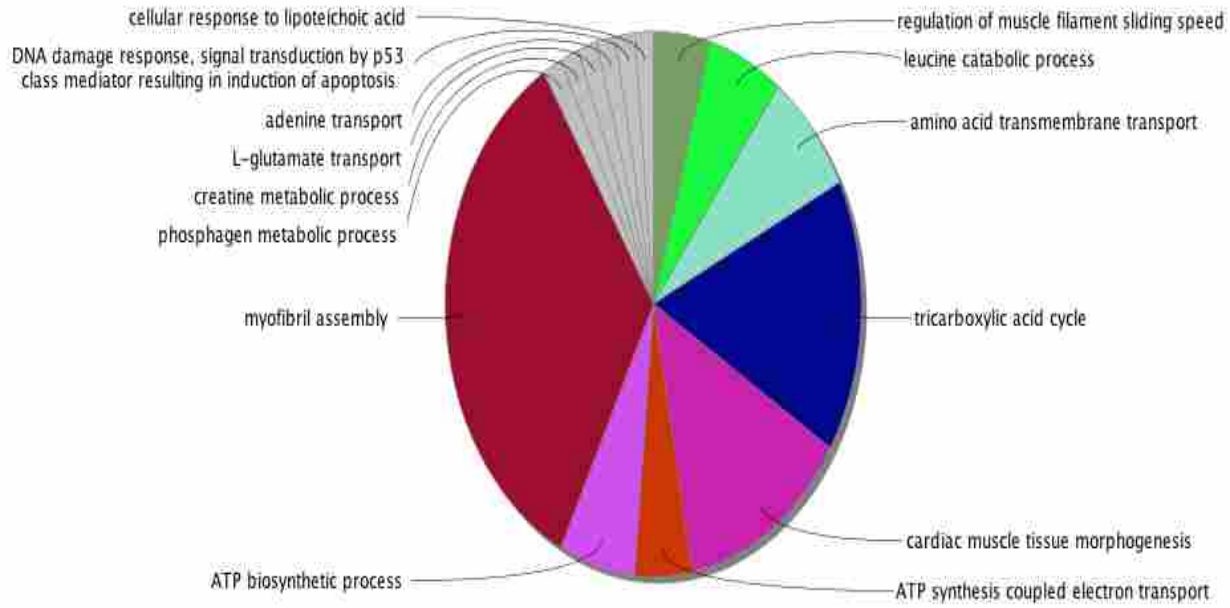
cellular response to lipoteichoic acid
DNA damage response, signal transduction by p53 class mediator resulting in induction of apoptosis
adenine transport
L-glutamate transport
creatine metabolic process
phosphagen metabolic process
myofibril assembly
ATP biosynthetic process
regulation of muscle filament sliding speed
leucine catabolic process
amino acid transmembrane transport
tricarboxylic acid cycle
cardiac muscle tissue morphogenesis
ATP synthesis coupled electron transport

F.

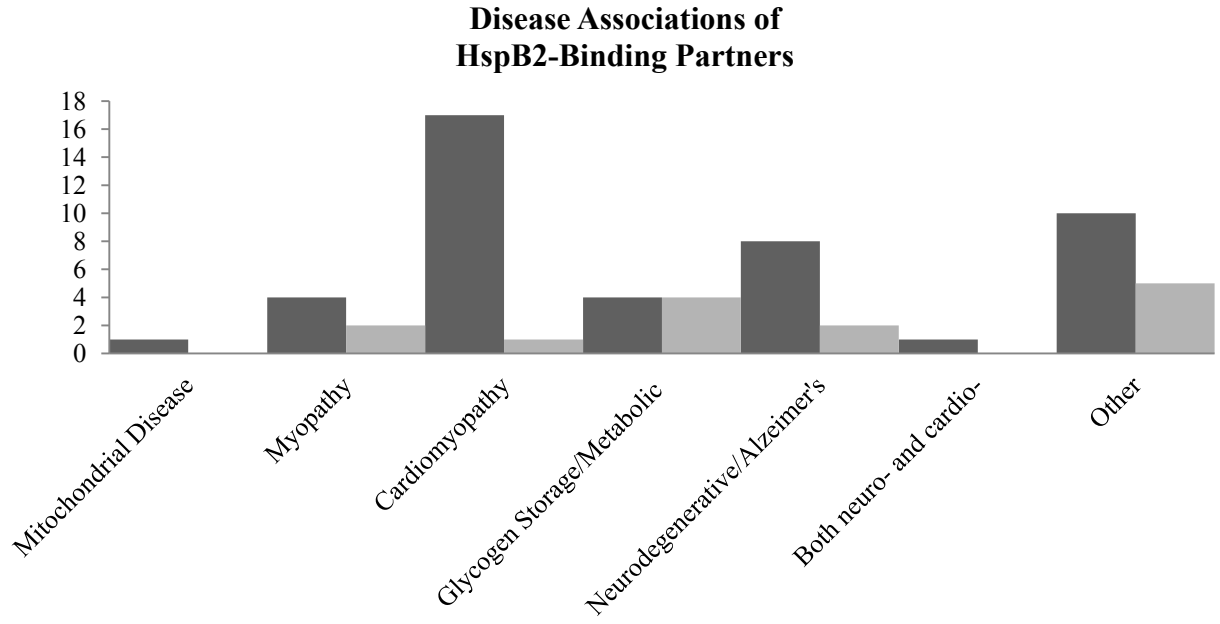

Figure 2.3. Network analysis of the HspB2 binding partners reveals direct protein-protein interactions. Known interactions between the HspB2 binding partners were mapped and identified using Cytoscape and the Uniprot, HPRD and BioGrid databases. (**A**) Protein network displaying known interactions between the HspB2 binding partners only. Created using Cytoscape [96]. Expanded protein network of Y2H (**B**) and mitochondrial copurification (**C**) results displaying direct protein-protein interactions from currently available human protein-protein interaction networks. Only proteins known to have direct interactions with the identified HspB2 binding partners are shown. (**D**) The combined expanded networks containing both the Y2H and mitochondrial copurification results and all known direct protein-protein interactions. (**E**) Analysis of the Y2H protein network using Gene Ontology analysis (Cytoscape ClueGO plugin [80]) revealing eight major pathways for HspB2 function. (**F**) Known Mendelian disease associations of HspB2 binding partners identified using the OMIM database. The darker bars represent HspB2-binding partners retrieved from the Y2H screen multiple times. The lighter bars represent HspB2-binding partners retrieved from the mitochondrial coimmunoprecipitation.

Network Analysis of the HspB2 Interactome Reveals Links to Myopathies and Neurodegenerative Disease.

Although the Y2H and mass spectroscopy screens performed in our study revealed proteins with a wide range of biological function, it was apparent that many of these proteins overlap in their biological pathway. In order to identify key pathways influenced by HspB2, the protein interaction network was expanded to include relevant direct protein-protein interactions from currently available human protein-protein interaction networks using Cytoscape [96]. Cytoscape identified 2,256 binary protein-protein interactions for the 143 multiple-hit Y2H binding partners (Figure 2.3B), and 1,896 for the 67 copurification binding partners (Figure 2.3C) and incorporated them on a combined HspB2 interaction network (Figure 2.3D). Detailed analysis of this network reveals eight major networks or pathways for HspB2 function, including myofibril assembly, tricarboxylic acid cycle, and cardiac muscle tissue morphogenesis, signifying the role HspB2 may play in maintaining the contractile structure of striated muscle as well as aerobic respiration (Figure 2.3E).

In addition to examining the major pathways of HspB2 function, the diseases associated with HspB2 binding partners were investigated. The 143 Y2H and 67 copurification binding partners are primarily associated with myopathies and neurodegenerative diseases such as Alzheimer's (Figure 2.3F). HspB2 is the only sHSP that has not been associated with a human disease. These results predict that alterations in HspB2 function may contribute to these diseases, consistent with previous reports of sHSPs found in Alzheimer plaques [97].

Comparison of HspB2 and CryAB Binding Partners Reveals Remarkable HspB2 Specificity.

Historically, sHSPs have been thought to be redundant, thus making study of individual function challenging. However, recent expression and phenotypic analysis has revealed unique functions suggesting these sHSPs may have differential clientele. In order to investigate the specificity of sHSPs, the binding affinity of HspB2 and the related sHSP CryAB was compared for 15 of the HspB2 binding partners recovered in the Y2H screen (Figure 2.4, Table 2.3). Remarkably, 9 of the 15 partners tested showed marked specificity for HspB2, with 6 binding both HspB2 and CryAB (including CryAB itself). This is the first demonstration of non-redundant clientele for these related sHSPs, supporting recent evidence of differential yet overlapping function.

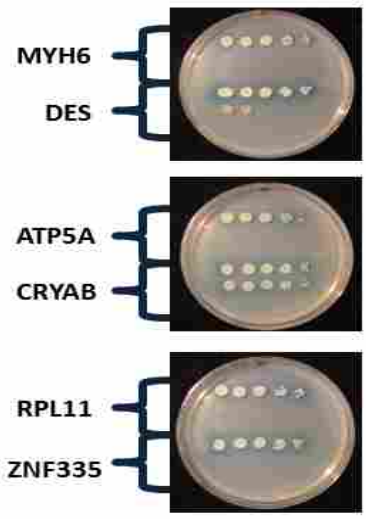

Figure 2.4. Comparison of HspB2 binding partners for HspB2 and the related sHSP CryAB reveals remarkable specificity for HspB2. Yeast two-hybrid (Y2H) assays for direct binding between HspB2 and 15 binding partners, 6 shown here, compared with direct binding to the related sHSP, CryAB. Y2H prey plasmids containing the indicated genes were transformed into Y2HGold (Contech) containing bait plasmids with either HspB2 (top row), CryAB (middle row), or an empty vector (bottom row). Overnight cultures were grown for 48 hours in SD-Trp-Leu to select for plasmids, then serially diluted and plated on SD-Trp-Leu-His-Ade plates to select for protein-protein interaction.

Table 2.3. Comparison of HspB2 binding partners for HspB2 and the related sHSP CryAB reveals remarkable specificity for HspB2.

Protein	HspB2	CryAB
ACAA2	Strong	No Growth
ALDOA	Strong	No Growth
ATP5A	Strong	No Growth
CRYAB	Strong	Strong
DES	Strong	Medium
DCTN1	Strong	No Growth
DZAP2	Strong	Strong
ENO3	Strong	Strong
EEF1A1	Strong	Strong
FTL	Strong	Strong
MYH6	Strong	No Growth
RPL11	Strong	No Growth
SDHA	Strong	No Growth
TTN	Strong	No Growth
ZNF335	Strong	No Growth

Fifteen binding partners from the HspB2 Interactome were tested for their ability to bind HspB2 or CryAB using the Y2H assay. The columns are as follows: the name of the gene encoded on the library plasmid retrieved from the Y2H screen, the Y2H result using HspB2 as bait, and the Y2H result using CryAB as bait. There was no growth when using the empty vector control for any of the binding partners tested.

Table 2.4. Putative HspB2 binding partners retrieved from the Y2H screen only once.

Signal Transduction				
Abhydrolase domain containing 12	Q8N2K0	ABHD12	Plasma Membrane	ND
Active breakpoint cluster region-related protein isoform a	Q12979	ABR	Cytoplasm	ND
ADP-ribosylhydrolase like 2	B7ZAN4	ADPRHL2	Mitochondria	ND
Adrenergic, beta, receptor kinase 1	P25098	ADRBK1	Cytoplasm	ND
Angiotensinogen (serpin peptidase inhibitor, clade A, member 8)	P21549	AGT	Extracellular	ND
Adenosylhomocysteinase-like 1	Q9BTL0	AHCYL1	Cytoplasm	ND
A-kinase (PRKA) anchor protein 13	Q12802	AKAP13	Plasma Membrane	ND
Annexin A11	P50995	ANXA11	Cytoplasm	ND
ArfGAP with RhoGAP domain, ankyrin repeat and PH domain 1	Q96P48	ARAP1	Golgi	ND
Calcium/calmodulin-dependent protein kinase II gamma	Q13555	CAMK2G	Cytoplasm	ND
Calcium modulating ligand	P49069	CAMLG	ER	ND
Chordin	Q9H2X0	CHRD	Extracellular	ND
V-crk sarcoma virus CT10 oncogene homolog (avian)-like	P46109	CRKL	Cytoplasm	ND
Dual specificity phosphatase 22	Q9NRW4	DUSP22	Cytoplasm	ND
Epidermal growth factor receptor pathway substrate 8	Q12929	EPS8	Cytoplasm	Yes
Fibroblast growth factor 12 isoform 2	P61328	FGF12	Nucleus	ND
Fms-related tyrosine kinase 1	P17948	FLT1	Plasma Membrane	ND
GRINL1A complex locus	H8Y6P7	GCOM1	Plasma Membrane	ND
Protein-coupled receptor kinase 5	P34947	GRK5	Plasma Membrane	ND
Protein HEG homolog 1	Q9ULI3	HEG1	Plasma Membrane	ND
Latrophilin 1	O94910	LPHN1	Plasma Membrane	ND
Latent-transforming growth factor beta-binding protein 1	Q14766	LTBP1	Extracellular	ND
MAD2L1 binding protein	Q15013	MAD2L1BP	Nucleus	ND
Mitogen activated protein kinase kinase kinase 10	Q02779	MAP3K10	Cytoplasm	ND
Mitogen-inducible gene 6 protein	Q9UJM3	MIG6	Cytoplasm	ND
Nuclear receptor coactivator 4	Q13772	NCOA4	Nucleus	ND
Nischarin	Q9Y2I1	NISCH	Plasma Membrane	ND
NODAL modulator 1	Q15155	NOMO1	ER	ND
NODAL modulator 2 or 3 (cannot distinguish)	Q5JPE7 P69849	NOMO2(3)		ND
Nephronectin	Q6UXI9	NPNT	Extracellular	ND
Atrial natriuretic peptide receptor 1 precursor	P16066	NPR1	Plasma Membrane	ND
Optineurin	Q96CV9	OPTN	Nucleus	ND
Platelet-derived growth factor beta polypeptide	P01127	PDGFB	Extracellular	ND
Phosphatidylethanolamine binding protein 1	P30086	PEBP1	Cytoplasm	ND
PTEN induced putative kinase 1	Q9BXM7	PINK1	Mitochondria	ND
Pleckstrin homology domain-containing family A member 7	Q6IQ23	PLEKHA7	Cytoplasm	ND
Protein phosphatase 2, catalytic subunit, beta isozyme	P62714	PPP2CB	Cytoplasm	ND
Protein kinase C, beta	P05771	PRKCB	Cytoplasm	ND
Protein kinase, DNA-activated, catalytic polypeptide	P78527	PRKDC	Nucleus	ND

Protein tyrosine phosphatase, non-receptor type 2	P17706	PTPN2	ER	ND
Protein tyrosine phosphatase, receptor type, M	A7MBN1	PTPRM	Plasma Membrane	ND
Rap guanine nucleotide exchange factor (GEF)-like 1	Q9UHV5	RAPGEFL1	Plasma Membrane	ND
Secreted frizzled-related protein 2	Q96HF1	SFRP2	Extracellular	Yes
SMAD family member 4	Q13485	SMAD4	Nucleus	ND
High endothelial venule protein	Q14515	SPARCL1	Extracellular	ND
Serine/threonine kinase 40	Q8N2I9	STK40	Nucleus	ND
Testis expressed 2	Q8IWB9	TEX2	Plasma Membrane	ND
Ubiquitin-like 5	Q9BZL1	UBL5	Cytoplasm	ND
Mitochondrial import stimulation factor L subunit	P62258	YWHAE	Cytoplasm	ND

Transcription Regulatory Protein				
Actin-like 6A	O96019	ACTL6A	Nucleus	ND
A-kinase anchor protein 6	Q13023	AKAP6	Nucleus	ND
AT-rich interactive domain-containing protein 4B isoform 1 and 2	Q4LE39	ARID4B	Nucleus	ND
cAMP responsive element binding protein 3	O43889	CREB3	ER	ND
DNA-damage-inducible transcript 3	P35638	DDIT3	Nucleus	ND
E2F transcription factor 6	O75461	E2F6	Nucleus	ND
Histone deacetylase 2	Q92769	HDAC2	Nucleus	ND
Helicase-like transcription factor	Q14527	HLTF	Nucleus	ND
High mobility group nuclosomal binding domain 2	P05204	HMGN2	Nucleus	ND
DNA-binding protein inhibitor ID-3	Q02535	ID3	Nucleus	ND
Intergrator complex subunit 4	Q96HW7	INTS4	Nucleus	ND
Intergrator complex subunit 10	Q9NVR2	INTS10	Nucleus	ND
KAT8 regulatory NSL complex subunit 3	Q9P2N6	KANSL3	Nucleus	ND
RNA polymerase-associated protein LEO1	Q8WVC0	LEO1	Nucleus	ND
Mbt domain containing 1	Q05BQ5	MBTD1	Nucleus	ND
Nuclear Factor I/A	Q12857	NFIA	Nucleus	ND
Nuclear factor I/X (CCAAT-binding transcription factor)	Q14938	NFIX	Nucleus	ND
Period circadian protein homolog 3	P56645	PER3	Nucleus	ND
PHD fingr protein 3	Q92576	PHF3	Nucleus	ND
Polymerase (RNA) II (DNA directed) polypeptide C, 33kDa	P19387	POLR2C	Nucleus	Yes
Polymerase (RNA) II (DNA-directed) polypeptide E 25 kDa	P19388	POLR2E	Nucleus	ND
Peroxisome proliferator-activated receptor alpha	Q07869	PPARA	Nucleus	ND
Peroxisome proliferative activated receptor gamma	P37231	PPARG	Nucleus	ND
RNA binding motif, single stranded interacting protein 1	P29558	RBMS1	Nucleus	ND
Ring finger protein 10	Q8N5U6	RNF10	Cytoplasm	ND
RuvB-like 2	Q9Y230	RUVBL2	Nucleus	ND
SET domain containing (lysine methyltransferase) 7	Q8WTS6	SETD7	Nucleus	ND
Staphylococcal nuclease domain containing 1	Q7KZF4	SND1	Nucleus	ND
Transcription factor 7-like 2 (T-cell specific, HMG-box)	Q9NQB0	TCF7L2	Nucleus	ND
Ubiquitin-conjugating enzyme E2 varient 2	Q15819	UBE2V2	Cytoplasm	ND
Zinc finger and BTB domain containing 16	Q05516	ZBTB16	Nucleus	ND
Zinc finger and BTB domain containing 38	Q8NAP3	ZBTB38	Nucleus	ND
Zinc Finger Protein 62 Homolog	Q8NB50	ZFP62	Nucleus	ND
Zinc Finger Protein, Multitype 2	Q8WW38	ZFPM2	Nucleus	ND
Zinc fingr protein 20	Q86XA2	ZNF20	Nucleus	ND
Zinc finger protein 232	Q9UNY5	ZNF232	Nucleus	ND
Zinc finger protein 333	Q96JL9	ZNF333	Nucleus	ND

Zinc finger protein 528	Q3MIS6	ZNF528	Nucleus	ND
Zinc finger family member 673	Q5JUW0	ZNF673	Nucleus	ND
Zinc finger protein 770	Q6IQ21	ZNF770	Nucleus	ND
Protein Biosynthesis and Processing				
Caprin family member 2	Q6IMN6	CAPRIN2	Cytoplasm	ND
Cyclin-dependent kinase 12	Q9NYV4	CDK12	Nucleus	ND
DnaJ (Hsp40) homolog, subfamily C, member 24	Q6P3W2	DNAJC24	Cytoplasm	ND
Exoribonuclease family member 3	O43414	ERI3	Nucleus	ND
Heterogeneous nuclear ribonucleoprotein A/B	Q99729	HNRNPAB	Nucleus	ND
Leucyl-tRNA synthetase	Q6NVI4	LARS	Mitochondria	ND
LSM domain-containing 1	Q9BRA0	LSMD1	Nucleus	ND
Mitrochondrial ribosomal protein L16	Q9NX20	MRPL16	Mitochondria	ND
Mitochondrial ribosomal protein L28	Q13084	MRPL28	Mitochondria	ND
Mitochondrial ribosomal protein L48	Q96GC5	MRPL48	Mitochondria	ND
Mitochondrial translation initiation factor 3	Q9H2K0	MTIF3	Mitochondria	Yes
Poly(rC) binding protein 1	Q15365	PCBP1	Mitochondria	ND
Peptidylprolyl isomerase E (cyclophilin E)	Q9UNP9	PPIE	Nucleus	ND
Peptidylprolyl isomerase F	P30405	PPIF	Mitochondria	ND
PRKR interacting protein 1	Q9H875	PRKRIP1	Nucleus	ND
Pseudouridylate synthase 3	Q9BZE2	PUS3	Nucleus	ND
KH domain containing, RNA binding	Q96PU8	QKI	Cytoplasm	ND
RNA binding protein fox-1 homolog 1	Q9NWB1	RBFOX1	Nucleus	ND
Ribosomal protein L3	P39023	RPL3	Cytoplasm	ND
Ribosomal protein L7	P18124	RPL7	Ribosome	ND
Ribosomal protein L8	P62917	RPL8	Nucleus	ND
Ribosomal protein L9	Q53Z07	RPL9	Ribosome	ND
Ribosomal protein L10a	P27635	RPL10	Ribosome	ND
Ribosomal protein L12	P30050	RPL12	Nucleus	ND
Ribosomal protein L26	P61254	RPL26	Ribosome	ND
Ribosomal protein L29	P47914	RPL29	Plasma Membrane	ND
Ribosomal protein S8	P62241	RPS8	Cytoplasm	ND
Ribosomal protein S18	P62269	RPS18	Ribosome	ND
Ribosomal protein S27 isoform	P62857	RPS27	Cytoplasm	ND
Ribosomal protein S28	P42677	RPS28	Ribosome	ND
Ribosomal RNA processing protein 1 homolog B	Q14684	RRP1B	Nucleus	ND
Small nuclear ribonucleoprotein polypeptide G	P62308	SNRPG	Nucleus	ND
Serine/arginine-rich splicing factor 3	P84103	SRSF3	Nucleus	ND
Tu translation elongation factor, mitochondiral	P49411	TUFM	Mitochondria	ND
Zinc finger, CCHC domain-containing protein 7	Q8N3Z6	ZCCHC7	Nucleus	ND
Fermentation/Respiration				
Aconitase 2	Q99798	ACO2	Mitochondria	ND
Alcohol dehydrogenase 1C (class 1), gamma polypeptide	P00326	ADH1C	Cytoplasm	ND
Cytochrome c oxidase subunit VIa polypeptide 2	Q02221	COX6A2	Mitochondria	ND
Cytochrome c oxidase subunit ViiC	P15954	COX7C	Mitochondria	ND
Cytochrome c oxidase assembly protein COX11, mitochondrial	Q9Y6N1	COX11	Mitochondria	ND
Enoyl CoA hydratase 1, peroxisomal	Q13011	ECH1	Peroxisome	ND
Enoyl-CoA hydratase/3-hydroxyacyl-CoA dehydrogenese	Q08426	EHHADH	Peroxisome	ND
Fission 1 (mitochondrial outer membrane) homolog 2	Q9Y3D6	FIS1	Mitochondria	ND
Galactose mutarotase (aldose 1-epimerase)	Q96C23	GALM	Cytoplasm	ND
Glutamic-oxaloacetic transaminase 1, soluble	P17174	GOT1	Cytoplasm	ND
Mitochondrial trifunctional enzyme, alpha subunit	P40939	HADHA	Mitochondria	ND

Hexokinase 1	P19367	HK1	Cytoplasm	ND
Isocitrate dehydrogenase (NADP)	O75874	IDH1	Cytoplasm	ND
Mannosidase, alpha, class 2B, member 2	O00754	MAN2B1	Lysosome	ND
Mitochondriall encoded cytochrome c oxidase subunit I	P00395	MT-CO1	Mitochondria	ND
NADH dehydrogenase (ubiquinone) 1 alpha subcomplex, 3, 9kDa	O95167	NDUFA3	Mitochondria	ND
NADH dehydrogenase (ubiquinone) 1 alpha subcomplex, 5	Q16718	NDUFA5	Mitochondria	ND
NADH dehyrdrogenase (ubiquinone) 1 alpha subcomplex, 8	P51970	NDUFA8	Mitochondria	Yes
NADH dehydrogenase (ubiquinone) 1 alpha, subcomplex 10	O95299	NDUFA10	Mitochondria	ND
NADH dehydrogenase (ubiquinone) 1 beta subcomplex	O95168	NDUFB4	Mitochondria	ND
Pyruvate dehydrogenase complex, component X	O00330	PDHX	Mitochondria	ND
Phosphoglycerate mutase 2 (muscle)	P15259	PGAM2	Cytoplasm	ND
Phosphoglycerate mutase family member 4	Q8N0Y7	PGAM4		ND
Succinate-CoA ligase, GDP-forming, beta subunit	Q96I99	SUCLG2	Mitochondria	ND
Ubiquinol-cytochrome c reductase core protein 1	P31930	UQCRC1	Mitochondria	Yes
Ubiquinol-cytochrome c reductase, Rieske iron-sulfur polypeptide 1	P47985	UQCRFS1	Mitochondria	ND
Myofibril or Cytoskeleton Structure/Regulation				
Actinin, alpha 1	P12814	ACTN1	Cytoplasm	Yes
ADAM metallopeptidase domain 23	O75077	ADAM23	Plasma Membrane	Yes
Desimin	P17661	DES	Cytoplasm	Yes
Dynein heavy chain domain 1	Q96M86	DNHD1	Cytoskeleton	ND
Adenylyl cyclase-associated protein 1	Q01518	CAP1	Cytoplasm	ND
Calponin 2	Q99439	CNN2	Cytoplasm	ND
Centrobin, centrosomal BRCA2 interacting protein	Q8N137	CNTROB	Cytoskeleton	ND
Gelsolin	P06396	GSN	Extracellular	ND
Kinesin family member 26A	Q9ULI4	KIF26A	Cytoskeleton	ND
LIM domain binding 3	O75112	LDB3	Cytoplasm	ND
Microtubule-associated protein 1B	P46821	MAP1B	Cytoplasm	ND
Marvel domain containing 1	Q9BSK0	MARVELD1	Plasma Membrane	ND
Myosin, heavy chain 9, non-muscle	P35579	MYH9	Cytoplasm	ND
Mysoin 1C	O00159	MYO1C	Plasma Membrane	Yes
Myosin IIIa	Q8NEV4	MYO3A	Cytoplasm	ND
Protein phosphatase 1, regulatory (inhibitor) subunit 12B	Q6GQY8	PPP1R12B	Cytoplasm	ND
RCSD domain containing 1	Q6JBY9	RCSD1	Cytoskeleton	ND
Septin 4	O43236	SEPT4	Mitochondria	ND
Sarcoglycan, delta (35kDa dystrophin-associated glycoprotein)	Q92629	SGCD	Plasma Membrane	ND
Synemin, intermediate filament protein	O15061	SYNM	Cytoskeleton	ND
Synaptopodin 2	Q9UMS6	SYNPO2	Cytoskeleton	ND
Troponin I type 1 (skeletal, slow)	P19237	TNNI1	Cytoplasm	ND
Utrophin	P46939	UTRN	Cytoplasm	ND
Small Molecule Biosynthesis and Catabolism				
4'-phosphopantetheinyl transferase	Q9NRN7	AASDHPPT	Cytoplasm	ND
Acylglycerol kinase	Q53H12	AGK	Plasma Membrane	ND
Glycerol-3-phosphate acytltransferase 3	Q53EU6	AGPAT9	ER	ND
Aldehye dehydrogenase 1 family, member L1	O75891	ALDH1L1	Cytoplasm	ND

Branched chain amino-acid transaminase 2, mitochondrial	O15382	BCAT2	Mitochondria	ND
CDP-diacylglycerol synthase	O95674	CDS2	Mitochondria	ND
Cytochrome P450, family 4, subfamily B, polypeptide 1	P13584	CYP4B1	ER	Yes
7-dehydrocholesterol reductase	Q9UBM7	DHCR7	Peroxisome	ND
Enolase superfamily member 1	Q7L5Y1	ENOSF1	Mitochondria	ND
High density lipoprotein binding protein	Q96CF6	HDLBP	Cytoplasm	ND
Hydroxysteroid (17-beta) dehydrogenase 3	Q5U0Q6	HSD17B3	ER	ND
Iron-sulfur cluster assembly factor homolog	Q5T440	IBA57	Mitochondria	ND
Ornitine aminotransferase	P04181	OAT	Mitochondria	ND
Phosphate cytidylyltransferase 2, ethanolamine	Q99447	PCYT2	Cytoplasm	ND
Procollagen-lysine, 2-oxoglutarate 5-dioxygenase 1	Q02809	PLOD1	ER	ND
Phosphopantothenoylcysteine decarboxylase	Q96CD2	PPCDC	Cytoplasm	ND
Retinol saturase (all-trans-retinol 13,14-reductase)	Q6NUM9	RETSAT	ER	ND
Serine hydroxymethyltransferase 2 (mitochondrial)	P34897	SHMT2	Mitochondria	ND
Trimethyllysine hydroxylase, epsilon	Q9NVH6	TMLHE	Mitochondria	ND
Thiopurine S-methyltransferase	P51580	TPMT	Cytoplasm	ND
Protein Degradation				
Cathepsin F	Q9UBX1	CTSF	Lysosome	ND
Cathepsin K	P43235	CTSK	Extracellular	ND
Cullin 5	Q93034	CUL5	Cytoplasm	ND
DDB1 and CUL4 associated factor 8	Q5TAQ9	DCAF8	Nucleus	ND
F-box protein, helicase, 18	Q66K33	FBXO18	Cytoplasm	ND
F-box and WD repeat domain containing 7, E3 ubiquitin protein ligase	Q969H0	FBXW7	Nucleus	ND
HtrA serine peptidase 1	Q92743	HTRA1	Extracellular	ND
Integral membrane protein 2B	Q9Y287	ITM2B	Plasma Membrane	ND
E3 ubiquitin-protein ligase NEDD4-like	Q96PU5	NEDD4L	Plasma Membrane	ND
Negative regulator of ubiquitin-like proteins 1	Q9Y5A7	NUB1	Nucleus	ND
Pitrilysin metallopeptidase 1	Q5JRX3	PITRM1	Extracellular	ND
Proteasome (prosome, macropain) subunit, beta type, 8	P28062	PSMB8	Cytoplasm	Yes
Ring finger protein 7	Q9UBF6	RNF7	Nucleus	ND
Selenium binding protein 1	Q13228	SELENBP1	Cytoplasm	ND
Ubiquitin A-52 residue ribosomal protein fusion product 1	P62987	UBA52	Ribosome	ND
Ubiquitin C	P0CG48	UBC	Cytoplasm	ND
Ubiquitin ligase E3B	Q7Z3V4	UBE3B	Cytoplasm	ND
Ubiquitin protein ligase E3 component n-recognin 2	Q8IWV8	UBR2	Nucleus	ND
Ubiquitin specific peptidase 9, X-linked	Q86X58	USP9X	Cytoplasm	ND
Cell Adhesion				
Multicatalytic endopeptidase complex subunit C13	O75339	PSMB8	Extracellular	ND
Collagen, type I, alpha 2	P08123	COL1A2	Extracellular	ND
Collagen, type XXIII, alpha-1	Q86Y22	COL23A1	Plasma Membrane	ND
Protocadherin 23	Q6V1P9	DCHS2	Plasma Membrane	ND
Desmoplakin	P15924	DSP	Cytoplasm	Yes
Elastin microfibril interfacer 2	Q9BXX0	EMILIN2	Extracellular	ND
Integrin alpha FG-GAP repeat containing 3	Q9H0X4	ITFG3	Plasma Membrane	ND
Integrin, beta 1	P05556	ITGB1	Plasma Membrane	ND

Laminin, alpha 2	P24043	LAMA2	Extracellular	Yes
Nexilin (F actin binding protein)	Q8NBZ9	NEXN	Plasma Membrane	ND
Thrombospondin, type 1, domain-containing 4	Q6ZMP0	THSD4	Extracellular	ND
Tight junction protein 1	Q07157	TJP1	Extracellular	ND
Tensin 1	A1L0S7	TNS1	Plasma Membrane	ND
Intracellular Trafficking				
Golgi-associated, gamma adaptin ear containing, ARF binding protein 1	Q9UJY5	GGA1	Golgi	ND
Golgin A4	Q13439	GOLGA4	Golgi	ND
Gasdermin B	Q8TAX9	GSDMB	Cytoplasm	ND
Insulin-like growth factor 2 receptor	P11717	IGF2R	Plasma Membrane	ND
Lecin, mannose-binding, 1 featuring protein ERGIC-53 precursor	P49257	LMAN1	ER	ND
Lysosomal trafficking regulator	Q99698	LYST	Lysosome	ND
Sorting nexin 3	O60493	SNX3	Cytoplasm	ND
Vesicel-associated membrane protein 3	Q15836	VAMP3	Plasma Membrane	ND
Vesicle-associated membrane protein 7	P51809	VAMP7	Cytoplasm	ND
YKT6 v-SNARE protein	O15498	YKT6	ER	ND
Zinc finger, FYVE domain containing 20	Q9H1K0	ZFYVE20	Plasma Membrane	ND
Cell Death				
CLPTM1-like	Q96KA5	CLPTM1L	Plasma Membrane	ND
CASP2 and RIPK1 domain containing adaptor with death domain	P78560	CRADD	Cytoplasm	ND
Defender against cell death 1	P61803	DAD1	ER	ND
Family with sequence similarity 188, member A	Q9H8M7	FAM188A	Nucleus	ND
Hepatitis B virus X interacting protein	O43504	HBXIP	Cytoplasm	ND
LYR motif containing 1	O43325	LYRM1	Nucleus	ND
Melanoma antigen family D, 1	Q9Y5V3	MAGED1	Cytoplasm	Yes
MT-RNR2-like 8	P0CJ75	MTRNR2L8	Cytoplasm	ND
Pleckstring homology-like domain, family A, member 3	Q9Y5J5	PHLDA3	Cytoplasm	ND
Rab interacting lysosomal protein-like	Q5EBL4	RILPL1	Cytoplasm	ND
Transmembrane protein 123	Q8N131	TMEM123	Plasma Membrane	ND
Transport				
Aquaporin-7	O14520	AQP7	Plasma Membrane	ND
La ribonucleoprotein domain family, member 1	Q6PKG0	LARP1	Nucleus	ND
Membrane-associated ring finger (C3HC4) 2, E3 ubiquitin protein ligase	Q9P0N8	MARCH2	Lysosome	ND
Solute Carrier Family 41, member 1	Q8IVJ1	SLC41A1	Plasma Membrane	Yes
POM121 membrane glycoprotein	Q9P0N8	POM121	Nucleus	ND
Rab interacting lysome protein	Q96NA2	RILP	Lysosome	ND
Solute carrier family 2 (facilitated glucose transporter), member 3	P11169	SLC2A3	Plasma Membrane	ND
Solute carrier family 38, member 1	Q9H2H9	SLC38A1	Plasma Membrane	ND

Phosphodiesterase 4D interacting protein	Q5VU43	PDE4DIP	Golgi	ND
Osmoregulation				
ATPase, Na+/K+ transporting, alpha 1 polypeptide	P05023	ATP1A1	Plasma Membrane	ND
ATPase, Ca++ transporting, plasma membrane 4	P23634	ATP2B4	Plasma Membrane	ND
ATP synthase, H+ transporting mitochondrial F1 complex, gamma polypeptide 1, nuclear gene encoding mitochondrial protein	P36542	ATP5C1	Mitochondria	ND
ATPase, H+ transporting, lysosomal accessory protein 2	O75787	ATP6AP2	Plasma Membrane	ND
ATPase, class VI, type 11A	P98196	ATP11A	Plasma Membrane	ND
Dicarbonyl/L-xyulose reductase	Q7Z4W1	DCXR	Plasma Membrane	ND
FXYD domain containing ion transport regulator 6	Q9H0Q3	FXYD6	Plasma Membrane	ND
Solute carrier family 9 (sodium, hydrogen exchange), member 1	P19634	SLC9A1	Plasma Membrane	ND
Immune				
Armadillo repeat containing, X-linked 1	Q9P291	ARMCX1	Plasma Membrane	ND
Major histocompatibility complex, Class 1, A	Q29946	HLA-A	Plasma Membrane	ND
Major histocompatability complex, class 1, C	Q95HC2	HLA-C	Plasma Membrane	ND
Interferon-related developmental regulator 2	Q12894	IFRD2	Nucleus	ND
Interleukin-1 receptor-associated kinase 1	P51617	IRAK1	Mitochondria	ND
Lysine (K)-specific demthylase 5D	Q9BY66	KDM5D	Cytoplasm	ND
Macrophage erythroblast attacher	B4DVN3	MAEA	Plasma Membrane	ND
Thymocyte selection associated family member 2	Q5TEJ8	THEMIS2		ND
Oxidoreductive Stress				
Glutathione peroxidase 4 (phospholipid hydroperosidase)	P36969	GPX4	Mitochondria	ND
Glutathione S-transferase omega 1	P78417	GSTO1	Nucleus	ND
Methionine sulfoxide reductase B1	Q9NZV6	MSRB1	MSRB1	ND
Phytanoyl-CoA 2-hydroxylase	O14832	PHYH	Peroxisome	ND
Peroxiredoxin 6	P30041	PRDX6	Lysosome	ND
Selenoprotein W, 1	P63302	SEPW1	Cytoplasm	ND
Serine/threonine kinase 25	O00506	STK25	Golgi	ND
Thioredoxin reductase 1	Q16881	TXNRD1	Cytoplasm	ND
Nucleotide Metabolism				
Adenylosuccinate synthase like 1	Q8N142	ADSSL1	Cytoplasm	ND
Adenylate kinase 4	P27144	AK4	Mitochondria	ND
Branched chain keto acid dehydrogenase E1, alpha polypeptide	P12694	BCKDHA	Mitochondria	ND
Cytidine deaminase	P32320	CDA	Nucleus	ND
Bis (5'-adenosyl)-triphosphatase	P49789	FHIT	Nucleus	ND
IMP (inosine 5'-monophosphate) dehydrogenase 2	P12268	IMPDH2	Cytoplasm	ND
Nudix (nucleoside diphosphate linked moiety X)-type motif 7	P0C024	NUDT7	Peroxisome	ND

Chaperone				
Ankyrin repeat domain-condtianing protein 13C	Q8N6S4	ANKRD13C	ER	ND
BCL2-associated athanogene 3	O95817	BAG3	Cytoplasm	ND
Chaperon containing TCP1 subunit 8	Q7Z759	CCT8	Cytoplasm	ND
Cell division cycle 37 homolog (S. cerevisiae)	Q16543	CDC37	Cytoplasm	ND
DNAJ (Hsp40) homolog, superfamily B, member 1	P25685	DNAJB1	Cytoplasm	ND
Heat shock protein 90kDA alpha (cytosolic), class A member 1	P07900	HSP90AA1	Cytoplasm	ND
Iron and Copper Homeostasis				
Ferritin, heavy polypeptide 1	P02794	FTH1	Cytoplasm	ND
Ferritin light polypeptide	P02792	FTL	Cytoplasm	Yes
Iron-sulfur cluster assembly enzyme ISCU, mitochondrial	Q9H1K1	ISCU	Nucleus	Yes
Metallothionein 2A	P02795	MT2A	Nucleus	Yes
Replication/Recombination				
Kelch domain containing 3	Q8IVW5	KLHDC3	Cytoplasm	ND
Non-structural maintenance of chromosomes element 4 homolog A	Q9NXX6	NSMCE4A	Nucleus	ND
Replication protein A1, 70kDa	P27694	RPA1	Nucleus	ND
Unknown				
Aquaporin 7 pseudogene 4		AQP7P4		ND
Coiled-coil domain containing 130	P13994	CCDC130	Nucleus	ND
Contactn-associated protein-like 3B precursor	Q96NU0	CNTNAP3B	Plasma Membrane	ND
Cytochrome c oxidase assembly factor 6 homolog	Q5JTJ3	COA6	Mitochondria	ND
Beta/gamma crystallin domain-containing protein 3	Q68DQ2	CRYBG3		ND
Down syndrome critical region gene 6	P57055	DSCR6	Nucleus	ND
ER membrane protein complex subunit 2	Q15006	EMC2	Cytoplasm	Yes
Family with sequence similarity 193, member A	P78312	FAM193A	Nucleus	ND
Family with sequence similarity 214, member A	Q32MH5	FAM214A		ND
G0/G1 switch 2		GOS2	Golgi	ND
MAP7 domain containing 1	Q3KQU3	MAP7D1	Cytoplasm	ND
Methyltransferase like 2A	Q96IZ6	METTL2A		ND
Nuclear prelamin A recognition factor	Q9UHQ1	NARF	Nucleus	ND
Protein-L-isoaspartate O-methyltransferase domain containing 1	Q96MG8	PCMTD1	Cytoplasm	Yes
Ribosomal protein L3-like	Q92901	RPL3L	Cytoplasm	ND
Ribosomal protein S2 pseudogene 23		RPS2P23		ND
RNA pseudouridylate synthase domain containing 2	Q8IZ73	RPUSD2	Cytoplasm	ND
Suppressor of tumorigenicity 7	Q9Y561	ST7	Plasma Membrane	ND
Starch binding domain 1	O95210	STBD1	Plasma Membrane	ND
Tctex1 domain containing 2	Q8WW35	TCTEX1D2	Cytoplasm	ND
Tudor domain containing 10	Q5VZ19	TDRD10		ND
Transmembrane protein 143	Q96AN5	TMEM143	Mitochondria	ND
TRAF3IP2 antisense RNA 1 (non-protein coding)		TRAF3IP2-AS1		ND
Ubiquitin specific peptidase 32 pseudogene 2		USP32P2		ND
Von Willebrand factor A domain containing 8	A3KMH1	VWA8	Extracellular	ND
YTH domain containing 2	Q9H6S0	YTHDC2	Nucleus	ND
Putative protein kinase regulator				ND

The data in this table contains the following information sequentially: protein name, UniProt protein accession number, gene symbol, cellular localization reported on HPRD or Genecards, and the results of Hspb2 dependency tests where applicable. ND is not determined. Only hits retrieved from the screen once are shown.

CHAPTER THREE: Identification of WTCryAB and R120GCryAB Clientele Reveals R120G to Have Hyperactive Binding Activity and Aggregation with Clientele

ABSTRACT

In the previous chapters I provided evidence for the role of HspB2 as a chaperone and introduced binding partners. I have also provided evidence for the non-redundant functions of HspB2 and CryAB through protein interaction studies. In this chapter, I will verify a subset of the HspB2 binding partners and will focus on the differences between CryAB and the mutant variant R120GCryAB on clientele and behavior. In addition, I will examine the effects of a recently isolated human mutation in HspB2 on its chaperone ability.

INTRODUCTION

Small heat shock proteins (sHSPs) are molecular chaperones characterized by the presence of a conserved 'alpha-crystallin domain' located near the C-terminus [5]. These small proteins are able to oligomerize and bind to misfolded proteins to preserve proper fold and function, to prevent erroneous aggregation, and to transfer misfolded proteins to larger ATP-dependent heat shock proteins for refolding or subsequent degradation (for recent reviews see [16, 18]). The sHSPs HspB2 and CryAB (HspB5) are highly expressed in cardiac and skeletal muscle and play protective roles against a variety of cellular stressors including heat extremes and mechanical and oxidative/reductive stress. In the heart, they maintain mitochondrial function and reduce the effects of cardiac stress [49, 50, 78, 84, 87, 88].

Small heat shock proteins have been implicated in a variety of processes. Such processes include cytoskeletal assembly, remodeling and stabilization, actin and intermediate filament

dynamics, apoptosis inhibition, cellular redox state maintenance, modulation of membrane fluidity and vasorelaxation [6-17]. Little is known regarding the molecular mechanisms by which HspB2 and CryAB maintain and protect the heart, although it is likely that HspB2 and CryAB help to maintain cellular processes through chaperone activity. By further characterizing a subset of HspB2 and CryAB binding partners using *in vitro* chaperone activity assays, we can determine whether these sHSPs are preventing heat-induced aggregation and helping to maintain the function of these proteins.

Mutations in sHSPs may not only result in a loss of chaperone activity, but may increase the aggregation of misfolding proteins or cause other unknown cellular effects. HspB2/CryAB double knockouts in mice result in heart failure and myopathy, including an increased heart to body weight and defective myocardial relaxation. A mutation in the CryAB gene denoted R120GCryAB results in increased expression of glucose-6-phosphate (G6PDH), consequentially increased cellular levels of NADPH, and ultimately the NADPH-dependent inducement of cardiomyopathy in mice. Our lab has previously performed a yeast two-hybrid (Y2H) screen with R120GCryAB and is currently performing a yeast two-hybrid screen with wild type (WT) CryAB in order to determine molecular differences between these two proteins. We hypothesize that the mutated CryAB sHSP may not contain the same protein-affinities and have differential chaperone ability, acting instead to inhibit proper protein folding.

In order to test our hypothesis, we have performed *in vitro* chaperone activity assays comparing the chaperone behavior of CryAB and R120G. From our results, we posit a dysfunction of the R120G mutant in which it is binding a broader range of clientele, yet has reduced chaperone activity. In addition, we have compared the clientele of HspB2 and a recently isolated mutant, A177PHspB2. Preliminary results obtained utilizing the Y2H assay indicate that

A177PHspB2 does not bind to the same subset of proteins found to associate with wild type (WT) HspB2, suggesting a possible difference in cellular activity. The results of our chaperone assays further indicate that while A177PHspB2 may be able to prevent clientele aggregation during heat stress, the mutant loses the ability to preserve enzymatic function. Combined, these results further solidify non-redundant clientele for sHSPs and posit a mechanism of action for the disease-associated R120GCryAB and A177PHspB2 alleles.

METHODS

Yeast Two-Hybrid (Y2H) Screen

Yeast harboring a human cDNA Y2H prey library (Clontech) were mated to yeast harboring a full-length R120GCryAB bait plasmid using the standard Matchmaker mating protocol (Clontech) and plated on Y2H selection plates (SD-Trp-Leu+ Aureobasidin) that were then patched to alternate Y2H selection plates (SD-Trp-Leu-His-Ade) for phenotype validation through alternate transcriptional reporters (HIS and ADE). The library plasmid inserts were identified for colonies arising on the SD-Trp-Leu-His-Ade plates by colony PCR followed by sequencing and NCBI BLAST analysis.

R120GCryAB and WTCryAB Binding Partner Comparison

Yeast two-hybrid (Y2H) assays for direct binding between R120G and the 14 binding partners identified compared with direct binding to WTCryAB. Y2H prey plasmids containing the indicated genes were transformed into Y2HGold (Contech) containing bait plasmids with either R120G, CryAB, or an empty vector. Overnight yeast cultures were grown for 48 hours on SD-

Trp-Leu plates to select for plasmids and patched on SD-Trp-Leu-His-Ade plates to select for protein-protein interaction.

Protein Expression and Purification

Two mitochondrial proteins GAPDH and ENO3 were cloned into pet15b (Novagen) for expression and purification. Genes were amplified from Origene plasmids SC118869 (accession number NM_002046) and SC118914 (accession number NM_001976) respectively using the following primers, pJG3284 (ggccatatggggaaggtgaaggtcggagtc), pJG3285 (ggcggatccttactccttggaggccatgtgggc), pJG3038 (ggccatatggccatgcagaaaatctttgcccg), pJG3039 (ggcctcgagtcacttggccttcgggttac) and cloned into pet15b at the NdeI/BamHI and NdeI/XhoI sites respectively. HspB2 was subcloned from the HspB2 Y2H bait plasmid (pJG591) into pet15b at EcoRI/XhoI sites. CryAB was subcloned from the CryAB Y2H bait plasmid (pJG736D) into pet15b at EcoRI/XhoI sites. A177PHspB2 was produced by mutating the wild type HspB2 pet15b plasmid (pJG1009) using Strategenes QuikChange Lightning kit. R120GCryAB was subcloned from the R120G Y2H plasmid (pJG581) and cloned into pet15b. Expression vectors were introduced into BL21 DES E. coli. Overnights were allowed to grow for 3 hours at 37°C. Expression was induced by 0.5 mM ITPG for 5 hours at 37°C. Pelleted bacteria were then resuspended in lysis buffer: XWA (20mL 1M HEPES pH 7.4, 2.5mL 4M KCl, 1.5mL 1M MgCl2, 2mL 0.5M EDTA pH 8.0, 2mL 0.5M EGTA pH 8.0, 1mL 1M DTT added fresh, ddH2O to a liter, pH 7.4), 300 mM NaCl, 1 mM beta-mercaptoethanol, and Roche Complete Protease Inhibitor Cocktail). Cells were lysed using the Microfluidics M-110P homogenizer and debris pelleted at 15,000 rpm for 60 minutes. The supernates were incubated with 250 uL of Ni-NTA agarose (Qiagen) for 2-3 hours. Beads were pelleted, washed twice with 15-25 mL of lysis buffer

and then transferred to a column to be washed with 50 mL of lysis buffer containing 25 mM imidazole and 300mM NaCl. Protein was eluted three times per sample with 0.3 mL of lysis buffer containing 250 mM imidazole and 100 mM NaCl.

In vitro Chaperone Assay

Chaperone assays were conducted by incubating purified protein at high temperature (43°C) for 30 minutes in 40 mM HEPES-KOH buffer (pH 7.5) with a final GAPDH or ENO3 protein concentration of 25 μg/mL and final sHSP concentration of 100 μg/mL. Aggregates were then pelleted by centrifugation (13,000 rpm for 10 minutes in a microcentrifuge). Both supernate and pellet were analyzed by SDS-PAGE. Bands of the SDS-PAGE gel were analyzed using the BioRad Fluor-S MultiImager and supernate to pellet ratios calculated.

Enzymatic Activity Assay

Purified protein GAPDH was incubated either alone or with WTHspB2 or A177PHspB2 at high temperature (43°C) for 30 minutes in 40 mM HEPES-KOH buffer (pH 7.5) with a final GAPDH protein concentration of 25 μg/mL and final sHSP concentration of 100 μg/mL. Aggregates were then pelleted by centrifugation (13,000 rpm for 10 minutes in a microcentrifuge). Supernate was then incubated at room temperature in 0.015 M sodium pyrophosphate buffer (pH 8.5), 0.1 M DTT, 0.015M D-glyceraldehyde-3-phosphate, and either with or without 7.5 mM NAD+. UV absorbance of NADH produced was measured at 340nm using the Biochrom Libra S4 Visible spectrophotometer.

RESULTS

Y2H Screens Reveal Non-redundant Binding Partners for CryAB and R120GCryAB

Preliminary evidence for the overlap in HspB2 and CryAB binding partners suggest that they have overlapping, yet non-redundant binding partners (see Table 2.3). In order to further compare and contrast the clientele of HepB2 and CryAB, we performed a small-scale Y2H screen to identify CryAB binding partners (Whitney Hayes, unpublished results). Surprisingly, expressing CryAB in yeast dramatically decreased the ability of yeast mating and hence our ability to screen the Y2H library. We, therefore, tried a mutated version of CryAB, R120G, which has been well-studied in the scientific literature and does maintain some activity. Using this variant, we identified 14 proteins that interact with R120GCryAB (Table 3.1). Once binding partners were pulled from the screen, their binding to WTCryAB was assessed. Of these proteins, 64% were found to also associate with WTCryAB.

Table 3.1 Putative R120GCryAB binding partners retrieved from a Y2H screen.

Gene Name	R120GCryAB	WTCryAB
XIRP1	Strong Growth	Strong Growth
MARCO	Strong Growth	Strong Growth
CRYAB	Strong Growth	Strong Growth
MMADHC	Strong Growth	Weak
CDC123	Strong Growth	Weak
UQCRC1	Strong Growth	Weak
FTL	Strong Growth	Weak
ATP2A2	Strong Growth	None
DES	Strong Growth	None
ACTC1	Strong Growth	None
KCNH2	Strong Growth	None
HLA-H	Weak	Weak
AOC3	Weak	None
TNS1	Very Weak	Very Weak

The data in this table contains the following information sequentially: Gene name, relative binding strength to R120GCryAB, and relative strength to WTCryAB. Binding strength was assessed by the Y2H (data produced by Whitney Hayes, unpublished results).

In vitro Chaperone Assays Reveal Differences in Chaperone Behavior Between WTCryAB and R120GCryAB

In order to determine if WTCryAB and R120GCryAB display differential chaperone activity, we performed *in vitro* chaperone activity assays. Surprisingly, both were able to prevent the heat-induced aggregation of GAPDH and ENO3 (Figures 3.1A and D). However, the mutant R120GCryAB was not as efficient at preventing the heat-induced aggregation of either GAPDH or ENO3 (Figures 3.1B and E). Additionally, more R120G was found in the pelleted fraction (Figure 3.1C and F), suggesting that while R120G may still possess chaperone ability, its chaperone activity is lowered leading to aggregation with its clientele.

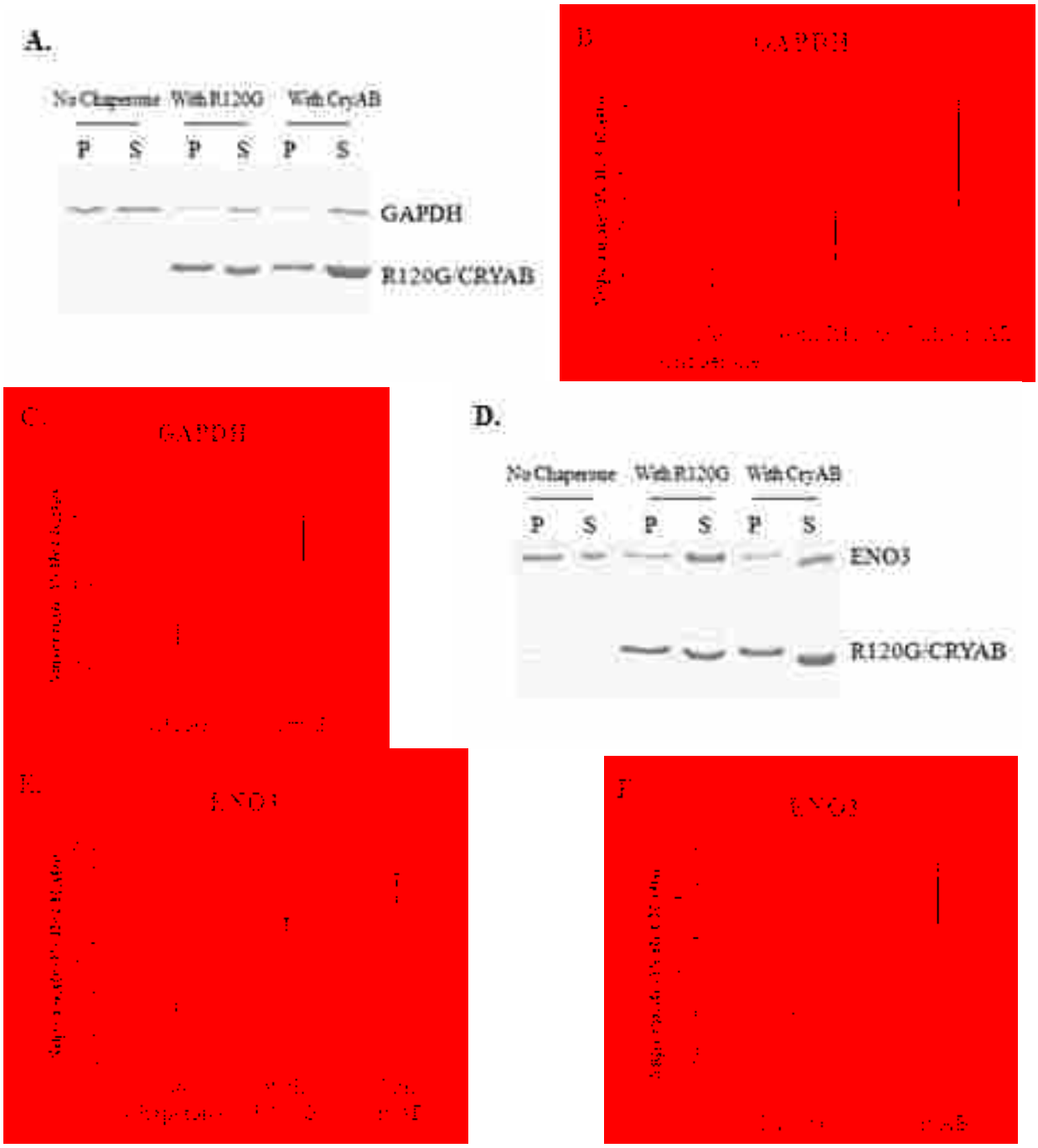

Figure 3.1. Analysis of CryAB and R120GCryAB chaperone activity towards the heat-induced aggregation of GAPDH and ENO3 reveals possible mechanisms of R120G-induced disease. The proteins GADPH (**A-C**) and ENO3 (**D-F**) were incubated with and without either CryAB or R120GCryAB and subjected to heat (43°C). Samples were assayed for denaturing by fractionation and SDS-PAGE analysis. Genes were cloned into pet15b (Novagen) then transformed into Bl21 DE3 for

expression and His-tag purification. Bands of the SDS-PAGE gel were analyzed using the BioRad Fluor-S MultiImager and supernate to pellet ratios calculated for the indicated assays (**B,C,E,F**). The supernates to pellet ratio for the chaperone alone (no substrate) is given in **C** and **F**.

Clientele Comparisons of WTHspB2 and A177PHspB2 Uncovers Altered Binding and an Eradicated Ability to Preserve Proper Clientele Function During Heat Stress

In collaboration with Dr. Keoni Kauwe, we recently identified a human variant of HspB2 in persons with Alzheimer's disease, A177PHspB2. This variant was a low frequency allele occurring in only 1 of 700 patients. In order to verify the functionality of this mutation, we tested its effects on both HspB2 clientele binding (Y2H) as well as *in vitro* chaperone activity. The A177P mutation abolished HspB2 binding to two independent binding partners as assessed by the Y2H (Figure 3.2). Surprisingly, however, the A177PHspB2 mutant had an increased ability to prevent the protein aggregation of both GAPDH and ENO3 under conditions of heat shock while still pelleting out itself to a greater extent than WTHspB2 (Figure 3.3). In order to test whether A177PHspB2 could preserve the enzymatic function of its clientele, we subjected heat-stressed GAPDH to an *in vitro* enzymatic activity assay and found that while HspB2 preserves GAPDH function, A177PHspB2 does not (Figure 3.4).

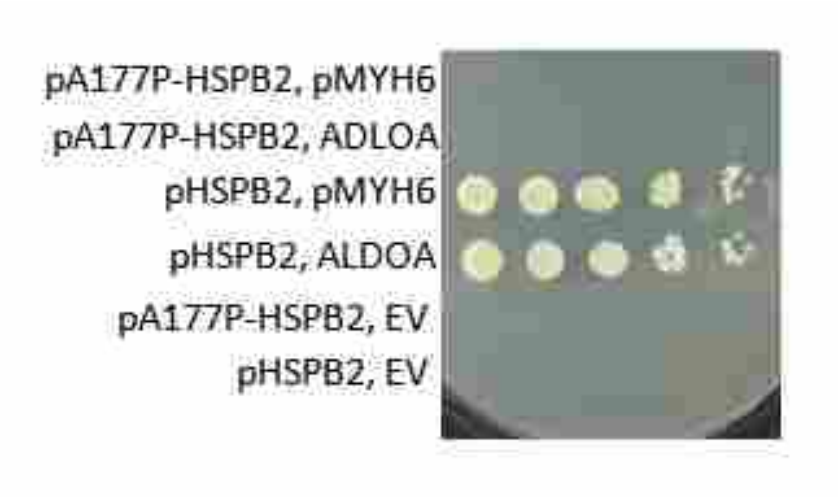

Figure 3.2. Unlike WTHspB2, the human mutant A177PHspB2 does not associate with ALDOA or MYH5. Yeast two-hybrid (Y2H) assays for direct binding between the recently identified human HspB2 mutant A177PHspB2 and the two HspB2-binding partners ALDOA and MYH5. Y2H prey plasmids containing the indicated genes were transformed into Y2H Gold (Clonetech) containing bait plasmids with either A177PHspB2, WTHspB2, or an empty vector. Overnight cultures were grown for 48 hours in SD-Trp-Leu to select for plasmids, then serially diluted and plated on SD- Trp-Leu-His-Ade plates to select for protein-protein interaction.

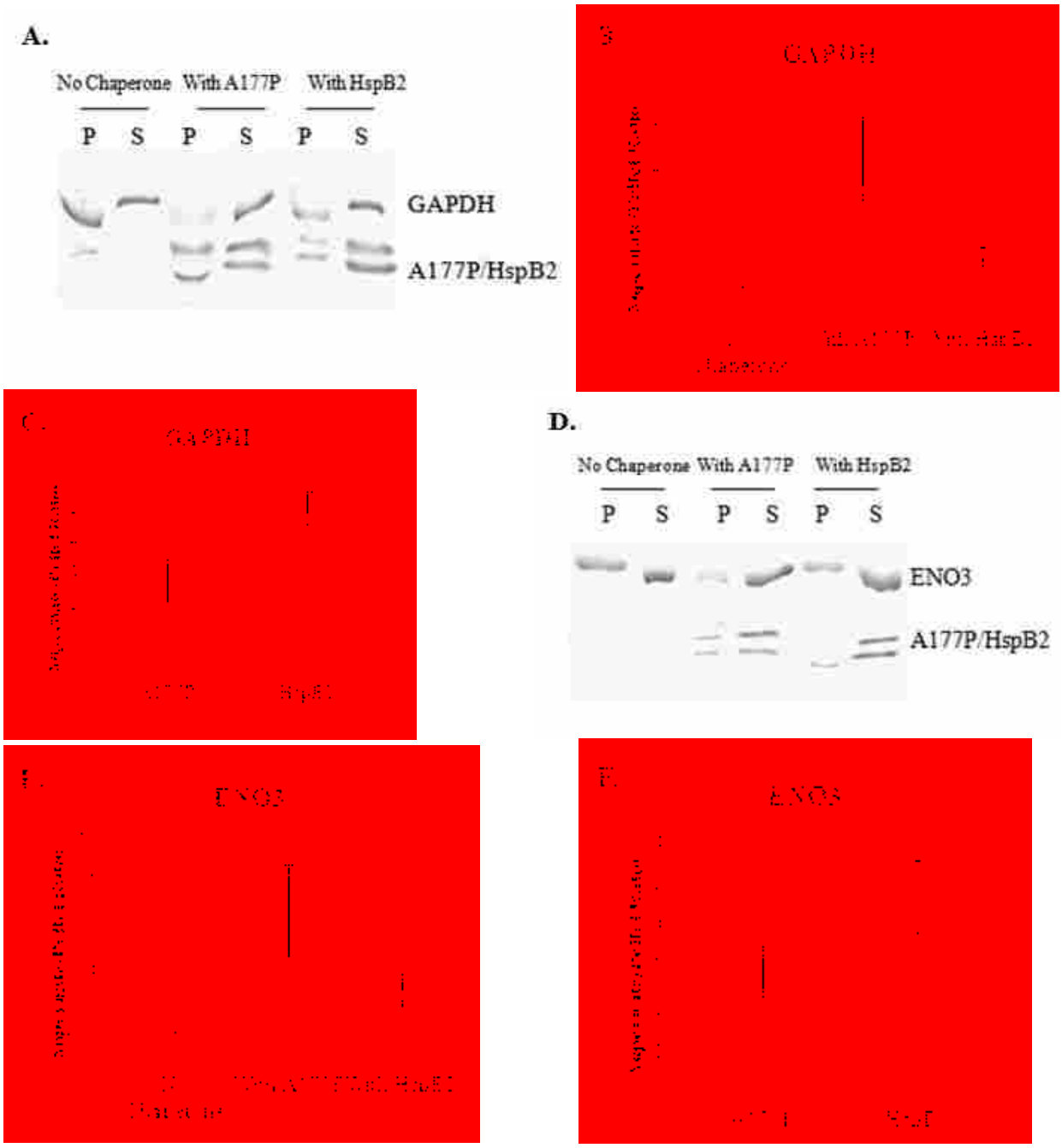

Figure 3.3. Analysis of WTHspB2 and A177PHspB2 chaperone activity towards the heat-induced aggregation of GAPDH and ENO3 reveals possible mechanisms of A177P-associated disease. The proteins GADPH (**A**) and ENO3 (**D**) were incubated with and without either WTHspB2 or A177PHspB2 and subjected to heat (43°C). Samples were assayed for denaturing by fractionation and SDS-PAGE analysis. Genes were cloned into pet15b (Novagen) then transformed into Bl21 DE3 for expression and

His-tag purification. Bands of the SDS-PAGE gel were analyzed using BioRad Fluor-S MultiImager and supernate to pellet ratios calculated for the indicated assays (**B,C,E,F**). The supernates to pellet ratio for the chaperone alone (no substrate) is given in **C** and **F**.

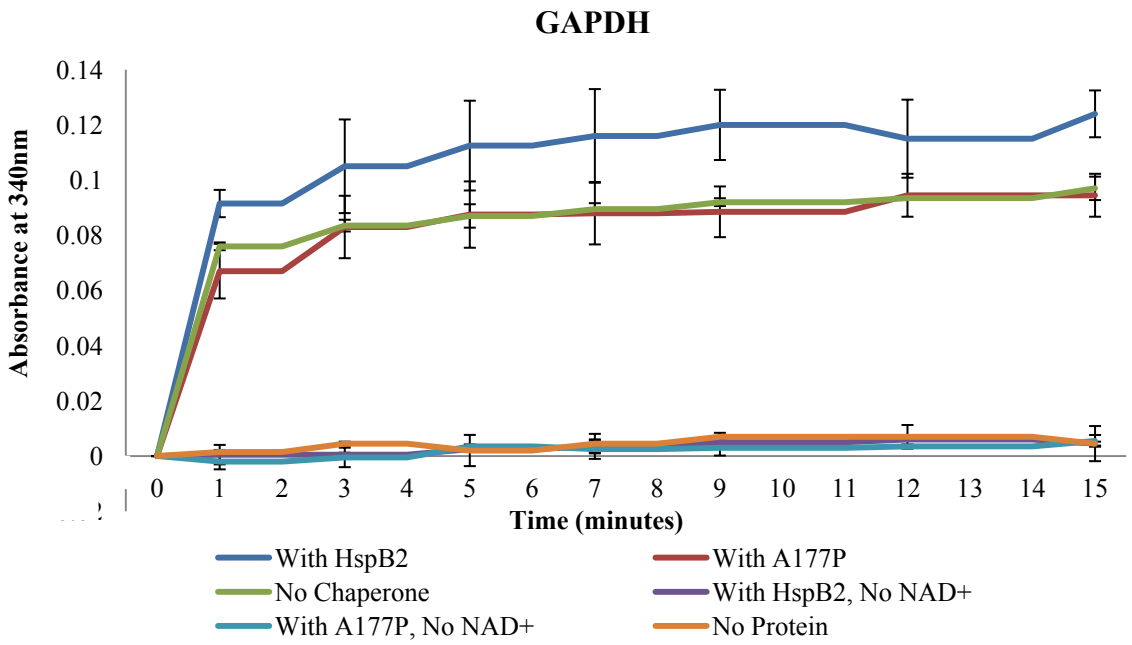

Figure 3.4. HspB2 and not A177PHspB2 preserves enzymatic activity of GAPDH. The protein GAPDH was incubated either alone or with WTHspB2 or A177PHspB2 and subjected to heat (43°C). The substrate D-glyceraldehyde-3-phosphate was then incubated with the heat-stressed samples (25°C) either with or without NAD+ and UV absorbance of NADH measured at 340nm.

CHAPTER FOUR: Summary and Discussions of Findings

The physiological importance of the family of sHSPs in human disease has been well established, however, their unique roles and molecular functions are just beginning to be unveiled [58, 60, 62]. Historically, the ten human sHSPs have been thought to be highly redundant, differing only in tissue expression patterns. The sHSPs CryAB and HspB2 appear to have arisen by genome duplication and are transcribed divergently on chromosome 11. While both CryAB and HspB2 are both expressed primarily in cardiac and skeletal muscle [68, 85], HspB2 is less studied. Although its importance in muscle physiology is clear, the precise molecular function of this protein remains unknown. In addition, despite the wealth of information available for CryAB, there remains a lack of understanding its *in vivo* clientele. Herein we described the first comprehensive search for HspB2 clientele and report the first evidence for non-redundant clientele. In addition, we characterize the clientele and chaperone activity of CryAB and an important human CryAB variant, denoted R120GCryAB, and propose a mechanism for its dysfunction.

Interestingly, HspB2 KO mice, but not CryAB KO mice, display defects in ATP production. Since no sHSP is known to function in the mitochondria, these effects on ATP production describe a novel function for HspB2 or may be secondary effects of cytoplasmic dysfunction. A key approach to understanding the function of any protein, perhaps especially a protein chaperone, is to identify the proteins with which it interacts. In the present study, an unbiased search for cardiac HspB2 binding partners using the frequented Y2H and copurification techniques reveals the first interactome for any sHSP as well as the first demonstration of mitochondrial clientele (see Chapter 2). These results are supported by *in vitro* chaperone

activity assays (see Figures 3.3 and 3.4). Furthermore, we demonstrate that CryAB binds less than 40% of the HspB2 interactome when assessed by Y2H. These results provide insight into the molecular mechanisms of HspB2 function and also establish a basis for contrasting the differential molecular roles of the sHSP family.

The primary cardiac HspB2 binding partners identified by Y2H were related to myofibril and mitochondrial function. The family of sHSP has long been known for stabilizing myofibril structure in both skeletal and cardiac sarcomeres and HspB2 is no exception [84, 85] The protein binding partners of HspB2, however, have been largely unknown with only DMPK [68] and HspB3 [86, 98] having been reported previously. Here we report over 200 novel HspB2 binding partners. Despite the large number of interacting partners identified, HspB2 interacted with less than 0.05% of the cardiac cDNA library suggesting specificity of target. In addition, only 6 of 15 binding partners tested also interacted with the related heat shock protein CryAB, suggesting specificity of function/clientele (see Table 2.3). This specificity is consistent with biochemical studies that indicate a unique structure for HspB2 when compared with CryAB [99].

Over 80% of the mitochondrial HspB2 binding proteins identified by Y2H were confirmed through HspB2 immunoprecipitation from cardiac mitochondria followed by quantitative mass spectroscopy (see Figure 2.2). The agreement between Y2H and quantitative mass spectroscopy approaches is remarkable given the large number of mitochondrial proteins [94, 95, 100] as well as the differences in the inherent advantages of each approach. Cardiac muscle has evolved to be highly resistant to fatigue due to the high proportion of mitochondria within each cardiomyocyte (estimated at 40% compared with 2% in skeletal muscle) [2]. Mitochondrial damage is prevalent under growth conditions that stimulate high respiration and this damage is thought to be the primary contributor to a large variety of human diseases including neurodegenerative diseases,

cardiovascular disorders, cancers and metabolic diseases [100-102]. Thus, stabilization of mitochondrial proteins by HspB2 may be a key factor in maintaining cardiac mitochondrial function, which explains the decrease in ATP production and phosphocreatine seen in HspB2-deficient mice [78]. In addition, transgenic over-expression of HspB2 leads to resistance to mitochondrial membrane permeability following cardiac stress (Ivor Benjamin, unpublished data), providing additional mitochondrial protection. Our results suggest that this protection is direct, that HspB2 binds to specific mitochondrial clientele.

The large number of mitochondrial targets isolated may come as no surprise since cardiac tissue is largely mitochondrial, however, no sHSP is known to reside in the mitochondria. This study revealed interactions between HspB2 and mitochondrial proteins encoded by both nuclear and mitochondrial DNA that reside in the mitochondria, supporting the possibility that HspB2 resides in the mitochondria. In support of our findings, HspB2 was previously shown to localize to the mitochondrial outer membrane in some cell lines [93], however, a mitochondrial association is not seen in mice, perhaps due to low levels of expression [78].

Although all other sHSPs have been found to play a role in various diseases including neurodegenerative and muscular disease, HspB2 has not been associated with a disease. The binding partners identified in this study suggest a role for HspB2 in neurodegenerative, mitochondrial, and muscular disease (see Figure 2.3). In support of this data, a dual knockout of CryAB and HspB2 was recently shown to enhance Alzheimer's phenotypes when crossed with Alzheimer's disease (AD) model mice [103]. In addition, HspB2 has recently been found in the senile plaques of Alzheimer's disease [97]. In collaboration with Dr. Keoni Kauwe, we were able to isolate two novel and rare HspB2 variants in Alzheimer's patients and show that one of these mutants, A177PHspB2, possesses a loss of protein-binding capacity *in vivo* (see Figure 3.2).

Additionally, while A177PHspB2 appears to have an enhanced ability to prevent clientele aggregation under conditions of heat stress, A177PHspB2 cannot preserve clientele enzymatic function (see Figure 3.3 and 3.4). This may be due to an increased clientele misfolding which could be caused by increased clientele dissociation affinity, thereby allowing A177PHspB2 to associate with clientele long enough to maintain solubility, but not long enough to preserve proper fold and function. In this way, the A177PHspB2 mutant has a loss of chaperone function and may be a contributing factor to the development of Alzheimer's disease.

The CryAB variant R120G is one of the most studied sHSP variant and causes cardiomyopathy in both humans and mice, however the precise mechanisms of its dysfunction have been unknown. We have shown using the Y2H assay that WTCryAB and R120GCryAB do not associate with the same binding partners and that R120G actually associates with a greater number of proteins (see Table 3.1). In addition, R120GCryAB possess a reduced chaperone activity for certain clientele under conditions of heat stress and aggregates to a greater extent with its substrates (see Figure 3.1). The R120G mutation may cause this sHSP to have a stronger binding affinity to clientele, causing R120GCryAB to bind tightly to clientele rather than binding and releasing. Our results support a model in which the R120G mutant displays hyper-binding activity and reduced chaperone activity, causing dysfunction by binding and sequestering proteins rather than preventing their stress-induced misfolding. These results, in addition to the results obtained for A177PHspB2, can help to elucidate the molecular mechanisms by which mutations in CryAB and HspB2 result in or contribute to disease.

Together, our findings provide the first comprehensive search for the clientele of any sHSP. Analysis of the comprehensive HspB2 protein interactome not only increases our understanding of HspB2, but provides a basis for studying its cellular effects and for comparing

its function to other sHSPs. In addition, our comparison of the HspB2 and CryAB clientele provide the first proof for non-redundancy in the molecular clientele of sHSPs and challenge the classic notion of non-specificity. Further comparisons of WTCryAB and the mutant R120GCryAB clientele have provided insight into the disease-causing mechanism of R120G. Finally, we present models for the molecular mechanisms of sHSP function in disease by comparing the chaperone abilities of wild type and mutant forms of both HspB2 and CryAB. These findings predict specific molecular roles for CryAB and HspB2 within the cell that should open up a field of future study. In addition, they predict specific mechanisms for the dysfunction of mutant HspB2 and CryAB forms that could be validated by further biochemical as well as *in vivo* analysis.

COMPLETE BIBLIOGRAPHY

1. Vliegen, H.W., et al., *Myocardial Changes in Pressure Overload-Induced Left-Ventricular Hypertrophy - A Study on Tissue Composition, Polyploidization and Multinucleation.* European Heart Journal, 1991. **12**(4): p. 488-494.
2. Ganong, W.F., *Review of medical physiology*. 13th ed. 1987, Norwalk, Conn.: Appleton & Lange. 665 p.
3. Tomohisa Nagoshi, M.Y., Giuseppe M. C. Rosano, Gary D. Lopaschuk, Seibu Mochizuki, *Optimization of Cardiac Metabolism in Heart Failure.* Current Pharmaceutical Design, 2011. **17**: p. 3846-3853.
4. Christians, E.S. and I.J. Benjamin, *Proteostasis and REDOX state in the heart.* American Journal of Physiology-Heart and Circulatory Physiology. **302**(1): p. H24-H37.
5. Guido Kappe, E.F., Pauline Verschuure, Wilbert C. Boelens, Jack A. M. Leunissen, Wilfried W. de Jong, *The human genome encodes 10 a-crystallin-related small heat shock proteins: HspB1-10.* Cell Stress and Chaperone, 2003. **8**(1): p. 53-61.
6. Wieske M, B.R., Behike J, Dolling R, Grelle G, Bielka H, Lutsch G, *Defined Sequence Segments of the Small Heat Shock Proteins Hsp25 and αβ-Crystallin Inhibit Actin Polymerization.* Eur j Biochem, 2001. **268**: p. 2083-2090.
7. Quinlan, R., *Cytoskeletal Competence Requires Protein Chaperones.* Prog Mol Subcell Biol, 2002. **28**: p. 219-234.
8. Arrigo, A.P., Paul C., Ducasse C., Manero F., Kretz-Remy C., Virot S., Javouhey E., Mounier N., Diaz-Latoud C., *Small stress proteins: Novel negative modulators of apoptosis induced independently of reactive oxygen species.* Prog Mol Subcell Biol, 2002. **28**: p. 185-204.
9. Tsvetkova NM, H.I., Torok Z, Wolkers WF, Balogi Z, Shigapova N, Crowe LM, Tablin F, Vierling E, Crowe JH, Vigh L, *Small Heat-Shock Proteins Regulate Membrane Lipid Polymorphism.* Proceedings of the National Academy of Sciences of the United States of America, 2002. **99**: p. 13504-13509.
10. Flynn CR, K.P., Tessier D, Thresher J, Niederkofler EE, Dreiza CM, Nelson RW, Panitch A, Joshi L, Brophy CM, *Transduction of biologically active motifs of the small heat shock-related protein HSP60 leads to relaxation of vascular smooth muscle.* FASEB Journal, 2003. **17**: p. 1358-1360.
11. Lavoie JN, H.E., Weber LA, Landry J, *Modulation of actin microfilament dynamics and fluid phase pinocytosis by phosphorylation of heat shock protein.* J Biol Chem, 1993. **268**: p. 24210-24214.
12. Benndorf R, H.K., Ryanzantsev S, Wieske M, Behlke J, Lutsch G, *Phosphorylation and supramolecular organization of murine small heat shock protein HSP25 abolish its actin polymerization-inhibiting activity.* J. Biol. Chem., 1994. **269**: p. 20780-20784.
13. Zhu Y, O.N.S., Salkatvala J, Tassi L, Mendelsohn ME, *Phosphorylated HSP27 associates with the activation-dependent cytoskeleton in human platelets.* Blood, 1994. **84**: p. 3715-3723.
14. RA, N.I.a.Q., *Chaperone activity of alpha-crystallins modulates intermediate filament assembly.* Embo Journal, 1994. **13**: p. 945-953.
15. Burfeind P, H.-F.S., *Structure and chromosomal assignment of a gene encoding the major protein of rat sperm outer dense fibres.* Eur J Biochem, 1993. **216**: p. 497-505.

16. Carra S, R.P., Crippa V, Giorgetti E, Boncoraglio A, Cristonfani R, Naujock M, Meister M, Minoia M, Kampinga H, Poletti A, *Different anti-aggregation and pro-degradative functions of the members of the mammalian sHSP family in neurological disorders.* Phil Trans R Soc B, 2013. **368**.
17. UP, A., *Crystallins in the eye: Function and pathology.* Progress In Retinal And Eye Research, 2007. **26**: p. 78-98.
18. Basha E, O.N.H., Vierling E, *Small heat shock proteins and α-crystallins: dynamic proteins with flexible functions.* Trends Biochem Sci, 2012. **37**(3): p. 106-117.
19. Kim, K.K., R. Kim, and S.-H. Kim, *Crystal structure of a small heat-shock protein.* Nature (London), 1998. **394**(6693): p. 595-599.
20. van Montfort R, B.E., Friedrich K, Slingsby C, Vierling E, *Crystal structure and assembly of a eukaryotic small heat shock protein.* Nature Structural Biology, 2001. **8**(12).
21. Bagneris C, e.a., *Crystal structure of alpha-crystallin domain dimers of alphaB-crystallin and Hsp20.* J. Mol. Biol., 2009. **392**: p. 1242-1252.
22. Jehle S, e.a., *AlphaB-crystallin: A hybrid solid-state/solution-state NMR investigation reveals structural aspects of the heterogeneous oligomer.* J. Mol. Biol., 2009. **385**: p. 1481-1497.
23. Herman Lambert, S.J.C., Andre´ F. Bernier, Alain Guimond, and Jacques Landry, *HSP27 Multimerization Mediated by Phosphorylation-sensitive Intermolecular Interactions at the Amino Terminus.* The Journal of Biological Chemistry, 1999. **274**(14): p. 9378-9385.
24. Ecroyd H, e.a., *Mimicking phosphorylation of alphaB-crystallin affects its chaperone activity.* Biochem. J., 2007. **401**: p. 129-141.
25. Akiko Iwaki, T.N., Midori Nakagawa, Toru Iwaki, Yasuyuki Fukumaki, *Identification and Characterization of the Gene Encoding a New Member of the a-Crystallin/Small hsp Family, Closely Linked to the aB-Crystallin Gene in a Head-to-Head Manner.* Genomics, 1997. **45**: p. 386-394.
26. Atsushi Suzuki, Y.S., Yukiko Hayashi, Nobuo Nyu-i, Michihiko Yoshida, Ikuya Nonaka, Sho-ichi Ishiura, Kiichi Arahata, Shigeo Ohno, *MKBP, a Novel Member of the Small Heat Shock Protein Family, Binds and Activates the Myotonic Dystrophy Protein Kinase.* The Journal of Cell Biology, 1998. **140**: p. 1113-1124.
27. Franck, E., et al., *Evolutionary diversity of vertebrate small heat shock proteins.* Journal of Molecular Evolution, 2004. **59**(6): p. 792-805.
28. Yuki Sugiyama, A.S., Masaru Kishikawa, Rika Akutsu, Tomonori Hirose, Mary M. Y. Waye, Stephan K. W. Tsui, Shosei Yoshida, Shigeo Ohno, *Muscle Develops a Specific Form of Small Heat Shock Protein Complex Composed of MKBP/HSPB2 and HSPB3 during Myogenic Differentiation* The Journal of Biological Chemistry, 2000. **275**: p. 1095-1104.
29. Jean Lud Cadet, M.T.M., Ning Sheng Cai, Irina N. Krasnova, Bruce Ladenheim, Genevieve and N.W. Beauvais, William Wood III, Kevin G. Becker, Amber B. Hodges, *Methamphetamine Preconditioning Alters Midbrain Transcriptional Responses to Methamphetamine-Induced Injury in the Rat Striatum.* PLoS ONE, 2009. **4**(11): p. 1-16.
30. Shama, K.M.A., et al., *Transient up-regulation of myotonic dystrophy protein kinase-binding protein, MKBP, and HSP27 in the neonatal myocardium.* Cell Structure and Function, 1999. **24**(1): p. 1-4.

31. Midori Nakagawa, N.T., Hiroyuki Nakagawa, Toru Iwaki, Yasuyuki Fukumaki, Akiko Iwaki, *Association of HSPB2, a Member of the Small Heat Shock Protein Family, with Mitochondria.* Experimental Cell Research, 2001. **271**: p. 161-168.
32. Takahiro Ishiwata, et al., *HSPB2 Is Dispensable for the Cardiac Hypertrophic Response but Reduces Mitochondrial Energetics following Pressure Overload In Mice.* PLoS ONE, 2012. **7**(8): p. 1-10.
33. Ilka Pinz, et al., *Unmasking different mechanical and energetic roles for the small heat shock proteins CryAB and HSPB2 using genetically modified mouse hearts.* The FASEB Journal, 2008. **22**: p. 84-92.
34. Ken-ichi Yoshida, T.A., Kazuki Harada, Kazi M.A. Shama, Yasuhisa Kamoda, Atsushi Suzuki, Shigeo Ohno, *Translocation of HSP27 and MKBP in Ischemic Heart.* Cel Structure and Function, 1999. **24**: p. 181-185.
35. Bogoyevitch MA, G.-B.J., Ketterman AJ, Fuller SJ, Ben-Levy R, Ashworth A, Marshall CJ, Sugden PH, *Stimulation of the Stress-Activated Mitogen-Activated Protein Subfamilies in Perfused Heart: p38/RK Mitogen-Activated Protein Kinases and c-Jun N-Terminal Kinases Are Activated by Ischemia/Reperfusion.* Circulation Research, 1996. **79**: p. 162-173.
36. Rouse J, C.P., Trigon S, Morange M, Alonso-Llamazares A, Zamanillo D, Hunt T, Nebreda AR, *A Novel Kinase Cascade Triggered by Stress and Heat Shock that Stimulates MAPKAP Kinase-2 and Phosphorylation of the Small Heat Shock Proteins.* Cell, 1994. **78**(6): p. 1027-1037.
37. Yoshida K, H.T., Akita Y, Mizukami Y, Yamaguchi K, Sorimachi Y, Ishihara T, Kawashima S, *Translocation of Protein Kinase C-α, δ, and ε Isoforms in Ischemic Rat Heart.* Biochem. Biophys. Acta, 1996. **1317**: p. 36-44.
38. Maizels ET, P.C., Kline M, et al., *Heat-Shock Protein-25/27 Phosphorylation by the Delta Isoform of Protein Kinase C.* Biochemical Journal, 1998. **332**: p. 703-712.
39. Huot J, H.F., Marceau F, Landry J, *Oxidative Stress-Induced Actin Reorganization Mediated by the p38 Mitogen-Activated Protein Kinase/Heat Shock Protein 27 Pathway in Vascular Endothelial Cells.* Circulation Research, 1997. **80**: p. 383-392.
40. Launay N, G.B., Kato K, Vicart P, Lilienbaum A, *Cell Signaling Pathways to αβ-Crystallin Following Stresses of the Cytoskeleton.* Experimental Cell Research, 2006. **312**(18): p. 3570-3584.
41. Sankaralingam Prabhu, et al., *HspB2/Myotonic Dystrophy Protein Kinase Binding Protein (MKBP) as a Novel Molecular Chaperone: Structural and Functional Aspects.* PLoS ONE, 2012. **7**(1).
42. den Engelsman, J., et al., *The Small Heat-Shock Proteins HSPB2 and HSPB3 Form Well-defined Heterooligomers in a Unique 3 to 1 Subunit Ratio.* Journal of Molecular Biology, 2009. **393**(5): p. 1022-1032.
43. Sun, X.K., et al., *Interaction of human HSP22 (HSPB8) with other small heat shock proteins.* Journal of Biological Chemistry, 2004. **279**(4): p. 2394-2402.
44. Unpublished data from the Grose Lab, 2013
45. Brady, J.P., et al., *alpha B-crystallin in lens development and muscle integrity: A gene knockout approach.* Investigative Ophthalmology & Visual Science, 2001. **42**(12): p. 2924-2934.

46. N. Golenhofen, A.R., E. F. Wawrousek, D. Drenckhahn, *Ischemia-induced increase of stiffness of aB-crystallin/HSPB2-deficient myocardium.* Eur J Physiol, 2006. **451**: p. 518-525.
47. Benjamin, I.J., et al., *CRYAB and HSPB2 deficiency alters cardiac metabolism and paradoxically confers protection against myocardial ischemia in aging mice.* Am J Physiol Heart Circ Physiol, 2007. **293**: p. H3201-H3209.
48. Lisa E. Morrison, R.J.W., Robert E. Klepper, Eric F. Wawrousek, and Christopher C. Glembotski, *Roles for aB-crystallin and HSPB2 in protecting the myocardium from ischemia-reperfusion-induced damage in a KO mouse model.* Am J Physiol Heart Circ Physiol, 2003. **286**: p. H847-H855.
49. Kadono, T., et al., *CRYAB and HSPB2 deficiency increases myocyte mitochondrial permeability transition and mitochondrial calcium uptake.* Journal Of Molecular And Cellular Cardiology, 2006. **40**(6): p. 783-789.
50. Kumarapeli, A.R.K., et al., *Alpha B-crystallin suppresses pressure overload cardiac hypertrophy.* Circulation Research, 2008. **103**(12): p. 1473-1482.
51. Kumarapeli, A.R.K., K. Horak, and X. Wang, *Protein quality control in protection against systolic overload cardiomyopathy: the long term role of small heat shock proteins.* American Journal Of Translational Research, 2010. **2**(4): p. 390-401.
52. Shayna E. Oshita, et al., *The small heat shock protein HspB2 is a novel anti-apoptotic protein that inhibits apical caspase activation in the extrinsic apoptotic pathway.* Breast Cancer Research and Treatment, 2010. **124**(2): p. 307-315.
53. Unpublished data from the Grose Lab, 2013
54. Acunzo, J., M. Katsogiannou, and P. Rocchi, *Small heat shock proteins HSP27 (HspB1), alphaB-crystallin (HspB5) and HSP22 (HspB8) as regulators of cell death.* Int J Biochem Cell Biol, 2012. **44**(10): p. 1622-31.
55. Boncoraglio, A., M. Minoia, and S. Carra, *The family of mammalian small heat shock proteins (HSPBs): implications in protein deposit diseases and motor neuropathies.* Int J Biochem Cell Biol, 2012. **44**(10): p. 1657-69.
56. Brownell, S.E., R.A. Becker, and L. Steinman, *The protective and therapeutic function of small heat shock proteins in neurological diseases.* Front Immunol, 2012. **3**: p. 74.
57. Chen, P., et al., *Alpha-crystallins and tumorigenesis.* Curr Mol Med, 2012. **12**(9): p. 1164-73.
58. Christians, E.S., T. Ishiwata, and I.J. Benjamin, *Small heat shock proteins in redox metabolism: implications for cardiovascular diseases.* Int J Biochem Cell Biol, 2012. **44**(10): p. 1632-45.
59. Clark, A.R., N.H. Lubsen, and C. Slingsby, *sHSP in the eye lens: crystallin mutations, cataract and proteostasis.* Int J Biochem Cell Biol, 2012. **44**(10): p. 1687-97.
60. Garrido, C., et al., *The small heat shock proteins family: the long forgotten chaperones.* Int J Biochem Cell Biol, 2012. **44**(10): p. 1588-92.
61. Ghayour-Mobarhan, M., H. Saber, and G.A. Ferns, *The potential role of heat shock protein 27 in cardiovascular disease.* Clin Chim Acta, 2012. **413**(1-2): p. 15-24.
62. Kampinga, H.H. and C. Garrido, *HSPBs: small proteins with big implications in human disease.* Int J Biochem Cell Biol, 2012. **44**(10): p. 1706-10.
63. Wettstein, G., et al., *Small heat shock proteins and the cytoskeleton: an essential interplay for cell integrity?* Int J Biochem Cell Biol, 2012. **44**(10): p. 1680-6.

64. Zoubeidi, A. and M. Gleave, *Small heat shock proteins in cancer therapy and prognosis.* Int J Biochem Cell Biol, 2012. **44**(10): p. 1646-56.
65. Golenhofen, N., et al., *Comparison of the small heat shock proteins alphaB-crystallin, MKBP, HSP25, HSP20, and cvHSP in heart and skeletal muscle.* Histochem Cell Biol, 2004. **122**(5): p. 415-25.
66. Kriehuber, T., et al., *Independent evolution of the core domain and its flanking sequences in small heat shock proteins.* FASEB J, 2010. **24**(10): p. 3633-42.
67. Laskowska, E., E. Matuszewska, and D. Kuczynska-Wisnik, *Small heat shock proteins and protein-misfolding diseases.* Curr Pharm Biotechnol, 2010. **11**(2): p. 146-57.
68. Suzuki, A., et al., *MKBP, a novel member of the small heat shock protein family, binds and activates the myotonic dystrophy protein kinase.* J Cell Biol, 1998. **140**(5): p. 1113-24.
69. Buchner, J., *Supervising the fold: functional principles of molecular chaperones.* FASEB J, 1996. **10**(1): p. 10-9.
70. Tyedmers, J., A. Mogk, and B. Bukau, *Cellular strategies for controlling protein aggregation.* Nat Rev Mol Cell Biol, 2010. **11**(11): p. 777-88.
71. van Montfort, R.L., et al., *Crystal structure and assembly of a eukaryotic small heat shock protein.* Nat Struct Biol, 2001. **8**(12): p. 1025-30.
72. Burbelo, P.D., G.R. Martin, and Y. Yamada, *Alpha 1(IV) and alpha 2(IV) collagen genes are regulated by a bidirectional promoter and a shared enhancer.* Proc Natl Acad Sci U S A, 1988. **85**(24): p. 9679-82.
73. Duncan, M.K., J.I. Haynes, 2nd, and J. Piatigorsky, *The chicken beta A4- and beta B1-crystallin-encoding genes are tightly linked.* Gene, 1995. **162**(2): p. 189-96.
74. Hudson, B.G., S.T. Reeders, and K. Tryggvason, *Type IV collagen: structure, gene organization, and role in human diseases. Molecular basis of Goodpasture and Alport syndromes and diffuse leiomyomatosis.* J Biol Chem, 1993. **268**(35): p. 26033-6.
75. O'Hanlon, T.P., N. Raben, and F.W. Miller, *A novel gene oriented in a head-to-head configuration with the human histidyl-tRNA synthetase (HRS) gene encodes an mRNA that predicts a polypeptide homologous to HRS.* Biochem Biophys Res Commun, 1995. **210**(2): p. 556-66.
76. Benjamin, I.J., et al., *CRYAB and HSPB2 deficiency alters cardiac metabolism and paradoxically confers protection against myocardial ischemia in aging mice.* Am J Physiol Heart Circ Physiol, 2007. **293**(5): p. H3201-9.
77. Golenhofen, N., et al., *Expression and induction of the stress protein alpha-B-crystallin in vascular endothelial cells.* Histochem Cell Biol, 2002. **117**(3): p. 203-9.
78. Ishiwata, T., et al., *HSPB2 is dispensable for the cardiac hypertrophic response but reduces mitochondrial energetics following pressure overload in mice.* PLoS One, 2012. **7**(8): p. e42118.
79. Kohl, M., S. Wiese, and B. Warscheid, *Cytoscape: software for visualization and analysis of biological networks.* Methods Mol Biol, 2011. **696**: p. 291-303.
80. Bindea, G., et al., *ClueGO: a Cytoscape plug-in to decipher functionally grouped gene ontology and pathway annotation networks.* Bioinformatics, 2009. **25**(8): p. 1091-3.
81. Fields, S. and O. Song, *A novel genetic system to detect protein-protein interactions.* Nature, 1989. **340**(6230): p. 245-6.
82. James, P., J. Halladay, and E.A. Craig, *Genomic libraries and a host strain designed for highly efficient two-hybrid selection in yeast.* Genetics, 1996. **144**(4): p. 1425-36.

83. Luban, J. and S.P. Goff, *The yeast two-hybrid system for studying protein-protein interactions.* Curr Opin Biotechnol, 1995. **6**(1): p. 59-64.
84. Pinz, I., et al., *Unmasking different mechanical and energetic roles for the small heat shock proteins CryAB and HSPB2 using genetically modified mouse hearts.* FASEB J, 2008. **22**(1): p. 84-92.
85. Yoshida, K., et al., *Translocation of HSP27 and MKBP in ischemic heart.* Cell Struct Funct, 1999. **24**(4): p. 181-5.
86. Sugiyama, Y., et al., *Muscle develops a specific form of small heat shock protein complex composed of MKBP/HSPB2 and HSPB3 during myogenic differentiation.* J Biol Chem, 2000. **275**(2): p. 1095-104.
87. Morrison, L.E., et al., *Roles for alphaB-crystallin and HSPB2 in protecting the myocardium from ischemia-reperfusion-induced damage in a KO mouse model.* Am J Physiol Heart Circ Physiol, 2004. **286**(3): p. H847-55.
88. Golenhofen, N., et al., *Ischemia-induced increase of stiffness of alphaB-crystallin/HSPB2-deficient myocardium.* Pflugers Arch, 2006. **451**(4): p. 518-25.
89. Stelzer, G., et al., *In-silico human genomics with GeneCards.* Hum Genomics, 2011. **5**(6): p. 709-17.
90. Magrane, M. and U. Consortium, *UniProt Knowledgebase: a hub of integrated protein data.* Database (Oxford), 2011. **2011**: p. bar009.
91. Cravatt, B.F., G.M. Simon, and J.R. Yates, 3rd, *The biological impact of mass-spectrometry-based proteomics.* Nature, 2007. **450**(7172): p. 991-1000.
92. Gavin, A.C., K. Maeda, and S. Kuhner, *Recent advances in charting protein-protein interaction: mass spectrometry-based approaches.* Curr Opin Biotechnol, 2011. **22**(1): p. 42-9.
93. Nakagawa, M., et al., *Association of HSPB2, a member of the small heat shock protein family, with mitochondria.* Exp Cell Res, 2001. **271**(1): p. 161-8.
94. Pohjoismaki, J.L., et al., *Postnatal cardiomyocyte growth and mitochondrial reorganization cause multiple changes in the proteome of human cardiomyocytes.* Mol Biosyst, 2013.
95. Zhang, J., et al., *Systematic characterization of the murine mitochondrial proteome using functionally validated cardiac mitochondria.* Proteomics, 2008. **8**(8): p. 1564-75.
96. Praneenararat, T., T. Takagi, and W. Iwasaki, *Integration of interactive, multi-scale network navigation approach with Cytoscape for functional genomics in the big data era.* BMC Genomics, 2012. **13 Suppl 7**: p. S24.
97. Gulick, J., et al., *Transgenic remodeling of the regulatory myosin light chains in the mammalian heart.* Circ Res, 1997. **80**(5): p. 655-64.
98. den Engelsman, J., et al., *The small heat-shock proteins HSPB2 and HSPB3 form well-defined heterooligomers in a unique 3 to 1 subunit ratio.* J Mol Biol, 2009. **393**(5): p. 1022-32.
99. Prabhu, S., et al., *HspB2/myotonic dystrophy protein kinase binding protein (MKBP) as a novel molecular chaperone: structural and functional aspects.* PLoS One, 2012. **7**(1): p. e29810.
100. Yang, J.S., et al., *Spatial and functional organization of mitochondrial protein network.* Sci Rep, 2013. **3**: p. 1403.

101. Pienaar, I.S., D.T. Dexter, and P.R. Burkhard, *Mitochondrial proteomics as a selective tool for unraveling Parkinson's disease pathogenesis.* Expert Rev Proteomics, 2010. **7**(2): p. 205-26.
102. Scharfe, C., et al., *Mapping gene associations in human mitochondria using clinical disease phenotypes.* PLoS Comput Biol, 2009. **5**(4): p. e1000374.
103. Ojha, J., et al., *Behavioral defects in chaperone-deficient Alzheimer's disease model mice.* PLoS One, 2011. **6**(2): p. e16550.